Heave, settlement and fracture of chalk during physical modelling experiments with temperature cycling above and below 0°C

Julian B. Murton[a,*], Jean-Claude Ozouf[b], Rorik Peterson[c]

[a]Permafrost Laboratory, Department of Geography, University of Sussex, Brighton BN1 9QJ, UK

[b]UMR 6143 du CNRS, "Morphodynamique Continentale et Côtière" M2C 24, rue des Tilleuls, 14000 Caen, France

[c]Department of Mechanical Engineering, University of Alaska, Fairbanks, USA

*Corresponding author: Tel.: +44 1273 678293; fax: +44 1273 876513 E-mail addresses: j.b.murton@sussex.ac.uk

Keywords : Physical modelling experiments, Rock heave and settlement, Fracture, Ice segregation, Permafrost

Abstract

To elucidate the early stages of heave, settlement and fracture of intact frost-susceptible rock by temperature cycling above and below 0°C, two physical modelling experiments were performed on 10 rectangular blocks 450 mm high of fine-grained, soft limestone. One experiment simulated 21 cycles of bidirectional freezing (upward and downward) of an active layer above permafrost, and the other simulated 26 cycles of unidirectional freezing (downward) of a seasonally frozen bedrock in a non-permafrost region. Heave and settlement of the top of the blocks were monitored in relation to rock temperature and unfrozen water content, which ranged from almost dry to almost saturated.

In the bidirectional freezing experiment, heave of the wettest block initially occurred abruptly at the onset of freezing periods and gradually during thawing periods (summer heave). After the crossing of a threshold marked by the appearance of a macrocrack in the upper layer of permafrost, summer heave increased by an order of magnitude as segregated ice accumulated incrementally in macrocracks, interrupted episodically by abrupt settlement that coincided with unusually high air temperatures. In the unidirectional freezing experiment, the wet blocks heaved during freezing periods and settled during thawing periods, whereas the driest blocks showed the opposite behaviour. The two wettest blocks settled progressively during the first 15 freeze-thaw cycles, before starting to heave progressively as macrocracks developed.

Four processes, operating singly or in combination in the blocks account for their heave and settlement: (1) thermal expansion and contraction caused heave and settlement when little or no water-ice phase change was involved; (2) volumetric expansion of water freezing in situ caused short bursts of heave of the outer millimetres of wet rock; (3) ice segregation deeper in the blocks caused sustained heave during thawing and freezing periods; and (4) freeze-thaw cycling caused consolidation and settlement of wet blocks prior to macrocracking in the unidirectional freezing experiment. Rock fracture developed by growth of segregated ice in microcracks and macrocracks at depths determined by the freezing regime. Overall, the heave, settlement and fracture behaviour of the limestone is similar to that of frost-susceptible soil.

1. Introduction

Near-surface bedrock, typically fractured, expands and contracts when subject to temperature cycles that cross the 0°C isotherm or take place at lower temperatures within permafrost. Vertical and/or horizontal movements of metamorphic and sedimentary bedrock have been measured in Arctic and Subarctic Canada (Dyke, 1984) and of igneous bedrock in southern Finland (Lehmuskoski et al., 2006; Hokkanen et al., 2007). Extension (during cooling) and contraction (during warming) of gneissic bedrock permafrost have been measured within rock walls in the Swiss Alps (Wegmann and Gudmundsson, 1999), and widening and narrowing of joints in sandstone, schist and shale monitored in the Swiss and Japanese Alps (Matsuoka, 2001, 2008). Expansion and contraction of bedrock can also occur by natural freezing behind tunnel linings (Kitagawa and Kawakami, 1984) and in excavations near artificially frozen ground (Smith et al., 2007). Bedrock movement produces various heave and weathering structures in present-day permafrost and periglacial regions (Dionne, 1983; Burn, 1984; Dredge, 1992), and brittle or ductile deformation structures in the upper 0.5–60 m of sedimentary rocks are common in some regions that hosted past permafrost, for example Great Britain (Hutchinson, 1991; Murton and Ballantyne, 2016). All of the observations cited above concern bedrock that contains joints or fractures. In present-day Arctic permafrost regions many fractures in bedrock contain ground ice, particularly in the upper metres of lithologies such as shale, arkose, schist and marly limestone, and some ice-filled fractures occur to depths of tens of metres in mountain or high-latitude permafrost (Gruber and Haeberli, 2007). However, the processes and their controlling factors involved in heave and fracture of bedrock newly subject to temperature cycling above and below 0°C have seldom been investigated (Murton et al., 2001, 2006) and remain to be examined in detail. Such investigation is important for studies of rock deformation and weathering, and for designing ground investigations and engineering structures because frost-susceptible bedrock is widespread in past and present periglacial regions.

Our aim here is to elucidate the early stages of heave and fracture of an intact frost-susceptible rock by temperature cycling above and below 0°C. We report observations from physical modelling experiments that investigated the heave and settlement of a single rock type subject to a wide range of moisture conditions and to ground thermal regimes that simulated (1) an active layer above permafrost and (2) seasonal freezing in a non-permafrost region. We used specimens of intact rock (i.e. that lacks visible joints and fractures) in order to identify macrofractures formed during temperature cycling. Our observations identify a variety of processes, operating singly or in combination that deform and fracture rock.

2. Experimental set-up

Two experiments were performed on ten rectangular blocks of frost-susceptible limestone (a French chalk known as ‘tuffeau’) 450 mm high and 300 mm x 300 mm wide, a size sufficient to simulate bedrock freezing almost at field scale. One experiment simulated bidirectional (upward and downward) freezing of a bedrock active layer above permafrost, and the other simulated unidirectional (downward) freezing of seasonally frozen bedrock in non-permafrost areas. The bidirectional experiment monitored four blocks (B1–B4) installed in a metal tank and insulated with polystyrene around their four vertical sides to minimize lateral heat conduction (Fig. 1A). Each block, on exposure to chilled air, froze from the top downward, simulating permafrost aggradation. After the freezing front had reached the bottom of the blocks, a basal cooling plate, thermostatically controlled, was switched on to maintain subzero temperatures (permafrost) in the lower part of each block for the remainder of the experiment. The upper part of each block was then cycled above and below 0°C, simulating thawing (summer) and freezing (winter) periods in the active layer. Thawing periods are defined by air temperatures >0°C

(allowing the upper part of the blocks to thaw from the surface downward), and freezing periods by air temperatures <0°C (allowing freezing downward from the surface and upward from the permafrost table). Twenty-one cycles of active-layer freezing and thawing were carried out. Freezing cycles averaged 5.47 days in duration (std dev. = 4.69 days), and thawing cycles averaged 12.87 ± 9.33 days. Values of active-layer thickness (*ALT*) were obtained by linear interpolation between temperature measurements to determine the maximum depth of penetration of the 0°C isotherm during thawing periods. The unidirectional freezing experiment monitored six blocks (U1–U6; Fig. 1B) during 26 freeze-thaw cycles, with freezing cycles averaging 6.36 ± 1.01 days, and thawing cycles 9.49 ± 6.58 days; it lacked a basal cooling plate, but was otherwise similar to the bidirectional experiment.

Different moisture conditions were maintained in the blocks in order to determine their effect on rock heave, fracture development and ice formation (Table 1 and Fig. 1). The blocks were initially dried in a desiccator at about 40°C prior to instrumenting and installing them in the metal tanks. Blocks B4 and U6 remained in their dried condition throughout the experiments, serving as controls. The other eight blocks were variably wetted by capillary rise. After capillary rise had finished in blocks B1, U1 and U2, they were placed on a bed of gravel with the water table about 10 mm above their base, allowing water to enter into the rock during the initial downward freezing of block B1 and during the late stages of each thawing cycle in blocks U1 and U2, resulting in wet conditions during the experiments. The other five blocks (B2, B3, U3, U4 and U5) were incompletely wetted by capillary rise and then isolated from the basal water table, resulting in intermediate water contents within them. Block U4 was sealed in a polythene sheet to prevent water from entering or leaving it during the experiment. Water was sprinkled onto the surface of all except for blocks U4, U6 and B4 during each thaw cycle, simulating summer rainfall.

Temperature in the air and rock, volumetric unfrozen water content in the rock, and heave of the block tops were measured during the experiments (Fig. 1). Rock temperature was measured by platinum resistance thermometers (100 Ω at 0°C) inserted at 50 mm intervals from the top to the base of blocks B1 to B4 (n = 10 per block) and from the surface to 350 mm depth in blocks U1 to U5 (n = 8 per block). Temperature in block U6 was measured by sensors at 0 to 250 mm and at 400 mm depth. Volumetric unfrozen water contents were measured by capacitance sensors inserted at 50 mm intervals from 50 to 400 mm depth in all 10 blocks (n = 8 per block). Heave of each block was measured by a linear variable differential transformer (LVDT) whose foot was glued to the centre of the top. Temperature and heave measurements were logged automatically at one-hour intervals, and water content was measured manually at intervals of some days. The measurements are described by Murton et al. (2006) and details of the instrumentation and rock type by Murton et al. (2000).

During the experiments, the instrumented side of the blocks was checked at variable intervals of time to determine if macrocracks had developed. At the end of the experiments, the blocks were extracted in frozen condition from their tanks and cracks within the blocks were examined and photographed.

3. Results

3.1. Air temperature

Air temperatures in the bidirectional freezing experiment had mean values of −5.8 to −4.3°C during freezing periods, and 14.3 to 22.5°C during thawing periods (Fig. 2A). Mean air temperatures for the unidirectional freezing experiment were −7.9 to −6.4°C during freezing periods and 14.8 and 24.4°C during thawing periods (Fig. 2B). Unusually warm air temperatures during thawing periods 18 and 19 in the former experiment and 22 in the latter peaked at 26.7 and 28°C, respectively, on 12 August 2003, during a heatwave in Europe (Schär et al., 2004).

3.2. Rock temperature

In the bidirectional freezing experiments the active layer cooled from the surface downward and from the permafrost table upward, and warmed from the surface downward. Cooling and warming in the wettest block (B1) were delayed relative to the driest (B4), as illustrated in Fig. 3A,C for two representative freezing and thawing periods. Temperature at and near the surface tended to be a few degrees °C higher during thawing periods in block B4 than in B1, and therefore temperature ranges between freezing and thawing periods were correspondingly greater in B4.

In the unidirectional freezing experiment the blocks cooled mainly from the surface downward, and warmed from the surface downward and from the bottom upward. Again, cooling and warming were delayed in the wettest block (U1) compared to the driest (U6), and surface temperature ranges were higher in the latter (Fig. 3D,F).

3.3. Water content

The water content in both experiments varied substantially between the wettest and driest blocks, particularly during thawing periods (Table 1). Mean values of volumetric unfrozen water content at the end of thawing periods (ϑ_{ut}) varied from 41 ± 6% in the active layer of block B1 to 8 ± 2% in that of B4, corresponding to % saturation of 86 ± 11 and 18 ± 4, respectively, while the underlying permafrost had low values of ϑ_{ut} (17 ± 4% in B1; 12 ± 1% in B4). Blocks B2 and B3 had ϑ_{ut} and % saturation values intermediate between those of B1 and B4. A similar range of values of ϑ_{ut} was determined for blocks U1 (45 ± 4%) to U6 (6 ± 1%). In contrast, mean volumetric unfrozen water content at the end of freezing periods (ϑ_{uf}) and % saturation dropped to values of between one third and two thirds of those for the thawing periods, apart for the dry block B4, whose values remained similar. The changes in water content for blocks B1 and U1 during two freeze-thaw cycles are illustrated in Fig. 3B,E. The unfrozen water content dropped as the active layer froze, with the minimum value occurring in the centre of the active layer (150 mm depth) at day 113 (Fig. 3B).

3.4. Active-layer thickness (ALT)

ALT values in blocks B1−B4 covaried with air temperature and showed variable relationships with water content during thawing periods (Table 2). The correlations between ALT and air temperature were higher with respect to maximum air temperature (r = 0.69–0.87) than to mean air temperature (r = 0.46–0.72). In both cases the relationship between *ALT* and air temperature become stronger as the water content in the blocks decreased. The correlations between *ALT* and ϑ_{ut} in the active layer switched signs from r = –0.51 in the wettest block (B1) to r = 0.44, 0.43 and 0.64 in the progressively drier blocks B2, B3 and B4, respectively.

The thickest active layer developed typically in the driest block (B4), and the thinnest active layer in the wettest block (B1; Fig. 2A). Unusually thick active layers developed during thawing period 19, which coincided with unusually high air temperatures caused by the heatwave of August 2003. During this thawing period, the typical relationship between ALT and water content reversed, with the wettest block (B1) having the thickest active layer and the driest block (B4) the thinnest. The reason for this reversed behaviour is not clear, although it may involve convective heat flow in the wettest blocks and air insulation in the driest.

The variation of *ALT* (ALT_{var}) increased with average water content of the blocks. ALT_{var} indicates the variation (range) between the thickest and thinnest active layers relative to the mean thickness:

$$ALT_{var} = \left(\frac{z_{max} - z_{min}}{z_{mean}}\right).100(\%) \quad (1)$$

where z_{max} is the maximum value of *ALT*, z_{min} the minimum value of *ALT* and z_{mean} the mean of *ALT*. Values of ALT_{var} are 48, 38, 32 and 16% for blocks B1, B2, B3 and B4, respectively, indicating that *ALT* varied most in the wettest block, and least in the driest (Fig. 2A).

3.5. Heave and settlement

3.5.1. Total net heave and total vertical strain

The overall change in elevation of the top of the unfrozen blocks measured during successive cycles of net heave (*total net heave*) was greatest (10.56 mm) for the wettest block (B1) in the bidirectional freezing experiment, intermediate in magnitude (2.39 mm) for block B2, and least for the two driest blocks (0.23 mm for B3; 0.30 mm for B4; Table S1). These values correspond to total vertical strains of 2.35, 0.53, 0.05 and 0.07% for B1 to B4, respectively. The maximum value of total net heave in the unidirectional freezing experiment was 0.73 mm in the wet block U2, equating to a total vertical strain of 0.16%, and the total net heave was substantially less in the other five blocks (Table S2).

3.5.2. Heave in freezing periods and thawing periods

Heave and settlement during freezing periods and thawing periods varied according to freezing regime, water content and the number of freeze-thaw cycles (Fig. 4; Tables S1 and S2). In the bidirectional freezing experiment the wettest block (B1) displayed the greatest mean heave (0.43 ± 0.20 mm) during freezing periods but the greatest variability of heave and settlement (mean heave = 0.10 ± 2.68 mm) during thawing periods. Thawing periods 1 to 9 were characterised by settlement that did not exceed –0.44 mm, but from thawing period 10 onward settlement increased by up to one order of magnitude (peaking at –8.54 mm in thawing period 18) and was replaced by heave of up to 6.19 mm in some thawing periods (Fig. 5A). Such variable behaviour is reflected in the high standard deviation (2.68 mm) in block B1 and the outliers in Fig. 4. Block B2 generally showed less variability, with heave not exceeding 0.21 mm during freezing periods and only small amounts of heave (up to 0.16 mm) or settlement (up to –0.21 mm) during thawing periods, until 2.13 mm of heave occurred in thawing period 21. Block B3 displayed minor settlement during all but one freezing period (mean = –0.09 ± 0.05 mm) and minor heave (mean = 0.11 ± 0.07 mm) during all but one thawing periods. Block B4 showed negligible heave or settlement during both freezing and thawing periods (mean = 0.00 ± 0.04 and 0.02 ± 0.06 mm, respectively).

In the unidirectional freezing experiment, the two wettest blocks (U1 and U2) also experienced the greatest mean values of heave and settlement, although values for U2 were greater during both freezing periods (1.56 ± 0.55 mm) and thawing periods (–1.49 ± 0.46 mm) than in U1 (1.13 ± 0.39 and –1.09 ± 0.31 mm, respectively; Table S2). In comparison, the four drier blocks (U3 to U6) showed mean values of

heave and settlement an order of magnitude or more lower; for example, the driest block (U6) experienced a mean value of just –0.12 ± 0.07 mm during freezing periods and 0.12 ± 0.08 during thawing periods. The sign of the relationship between freezing periods and mean heave switched (from positive to negative), and between thawing periods and mean settlement (from negative to positive) for blocks U3, U5 and U6 relative to blocks U1 and U2 (Fig. 4). Thus, U3, U5 and U6 tended to settle during freezing periods and heave during thawing periods, although the magnitudes were small.

Distinct trends in heave and settlement developed at different times in the unidirectional freezing experiment (Fig. 5C). Progressive settlement characterised the first 15 or so freeze-thaw cycles in blocks U1 and U2, prior to progressive heave that continued until the end of the experiment. Blocks U3 to U6 also showed progressive settlement, during the first two to three cycles, but thereafter showed no trend.

3.5.3. Bidirectional freezing time series of heave

Time series of heave and settlement also varied according to thermal regime, water content, the number of freeze-thaw cycles and the timing of macrocracking (Fig. 5). All four blocks subject to bidirectional freezing usually showed small but progressive heave of about 0.05–0.1 mm during active-layer thawing periods (Fig. 5B). Heave behaviour is classified into two stages for wet blocks B1 and B2. During the first stage, incremental heave alternated with bursts of early winter heave of about 0.2–0.6 mm at the beginning of active-layer freezing periods and similar bursts of early summer settlement at the beginning of active-layer thawing periods (Figs. 5B, 6A and 7A).

The second stage began when a threshold was crossed, after which the magnitude of heave during active-layer thaw increased by an order of magnitude. The threshold was about day 150 in B1 and day 368 in B2 (Fig. 5A), preceding heave totalling 4.6 mm in B1 and 2.1 mm in B2 during the remainder of the thawing period (Figs. 5A, 6B and 7B). Such summer heave encompassed the first observation, on day 166, of a subhorizontal macrocrack at a depth of 250 mm in B1, and a similar macrocrack was observed at a depth of 250–270 mm in B2 at the end of the experiment. We cannot exclude the possibility that the macrocrack in B1 developed several days before day 166. In both blocks, summer heave passed, with a small inflection, into a short period of early winter heave in freezing periods 11 in B1 (Fig. 6B) and 22 in B2 (Fig. 7B). Thereafter heave and settlement of B1 varied, as summer heave was episodically interrupted by settlement during some simulated late-summer conditions, when active-layer temperatures peaked (Fig. 6C). For example, abrupt settlement of nearly 10 mm on day 283 coincided with unusually high air temperatures. But summer heave during the next three thawing periods led to complete recovery of the block top to its pre-settlement elevation (Fig. 5A).

All blocks showed, at times, an in-phase relationship between heave and temperature. The relationship is clearly shown by the coincidence of minor (<0.1 mm) heave and settlement cycles with small (<3°C) rises and falls in the temperature at 400 mm depth, which were driven by the thermostatically-controlled basal cooling plate. The cycle frequency was about 1 day during thawing periods (Fig. 6A) and 4–5 days during freezing periods, the latter displaying a distinctive sawtooth pattern of gradual winter heave of about 0.1 mm preceding abrupt winter settlement of a similar amount (Figs. 8A and 9A). Independent of the cooling plate, additional winter settlement of about 0.1 mm coincided with rapid cooling of the rock following the zero curtain freezing conditions in B2 (e.g. freezing periods 4, 7 and 9; Fig. 7A) and B3 (freezing periods 2, 3 and 4; Fig. 8B). The in-phase relationship between heave and temperature in B3, however, changed to anti-phase during the heatwave in thawing periods 18 and 19. In both of these periods heave occurred initially as the rock warmed (Fig. 8C). But after day 282 in thawing period 18 and day 306 in thawing period 19, settlement commenced as the active layer deepened more than usual (Fig. 2A).

The abrupt bursts of heave and settlement that characterised the start of many freezing and thawing periods, respectively, in the wettest blocks B1 and B2 (Figs. 6 and 7A), occurred only occasionally in B3 and appeared to be absent in B4 (Fig. 9B,C). The rare occurrence of abrupt winter heave at the start of freezing period 6 in B3 (Fig. 8B) occurred when the upper 150 mm of the active layer was cooling but still above 0°C while the permafrost was also cooling, leading to upfreezing from the permafrost table. Likewise, settlement during heatwave conditions of thawing periods 18 and 19 was negligible in B4 (Fig. 9C) and minor (≤0.1 mm) in B3 (Fig. 8C) relative to B1 (Fig. 5A).

3.5.4. Unidirectional freezing time series of heave

In the unidirectional freezing experiment the two wettest blocks (U1 and U2) generally displayed the opposite heave and settlement behaviour to the drier blocks (U3 to U6; Fig. 5C). U1 and U2 heaved during freezing periods and settled during thawing periods. Freezing periods showed three stages of heave (stages 1 to 3), the first two marked by a distinct 'shoulder' on Fig. 10A,B: (1) rapid heave of about 0.1−0.6 mm began at the start of the freezing period and lasted for several hours, during freezing of the upper few tens to several tens of millimetres of rock; (2) slowing or cessation of heave, followed by zero heave or minor heave of about 0.1 mm in U1 and by minor settlement of a similar magnitude in U2, lasted about 1−3 days; and (3) rapid heave of about 0.8−2.0 mm re-commenced a few to several hours after the zero curtain phase ended at about 100 mm depth (and rapid freezing commenced at this depth) and terminated at the end of the freezing period, usually several days later. Stage 3 heave coincided with the zero curtain freezing at depths of 150 mm or more and its rate declined as the rock progressively froze.

Thawing periods in U1 and U2 showed either one or three stages of settlement (stages 4 to 6), the first two, where present, marked by a shoulder more subdued than the freezing shoulder (Fig. 10A,B): (4) rapid settlement of about 0.05−0.5 mm frequently occurred over a period of a few to several hours, as the rock warmed rapidly while the surface temperature remained below 0^{o}C; (5) slow settlement (or even heave of 0.1−0.2 mm during some thawing periods in U1) commenced with the start of zero curtain thawing and lasted about one day; and (6) rapid settlement re-commenced as thawing reached a depth of about 20−60 mm and slowed once thawing reached a depth of about 50−110 mm during the middle to later part of the zero curtain phase. The overall settlement during stage 6 was about 0.5−2.0 mm over about 4−5 days. In some cycles, stages 4 and 5 were absent. Settlement was followed by a period of stasis during the later part of the thawing period, when rock temperature exceeded 0^{o}C and thawing had finished.

The driest blocks U5 and U6 settled during freezing periods and heaved during thawing periods, at rates in proportion to rates of temperature change (Fig. 11B,C). Settlement of about 0.2 mm took place in over several days during freezing periods, and heave of a similar amount over several days during thawing periods. Interestingly, delayed cooling caused by zero curtain conditions during freezing of the lower part of U5 generally had little if any impact on the rate of settlement.

Blocks U3 and U4 showed more complex and variable behaviour during freeze-thaw cycles than U5 and U6. Some cycles in U3 showed a spike of rapid heave at the start of freezing periods (e.g. 16F in Fig. 10C). All showed some settlement during freezing and heave during rapid warming of rock post-thaw. U4 displayed a spike of rapid heave of about 0.1−0.2 mm at the start of freezing periods, often followed by rapid settlement as the block cooled rapidly. During zero curtain freezing little heave or settlement occurred. Warming of frozen rock prior to onset of zero curtain thaw was sometimes marked by a second, smaller spike in heave. Thereafter, settlement characterised the period of zero curtain thawing. Heave re-commenced once thawing was complete and the rock warmed rapidly.

3.6. Macrocracks and ground ice

Macrocracks developed in the four wettest blocks (B1, B2, U1 and U2) during the experiments (Figs. 12 and 13). By the end of the experiments, the cracks, typically horizontal to subhorizontal, were concentrated just beneath the permafrost table in B1 and B2 (Fig. 14), and mostly in the upper 15 cm of rock in U1 and U2 (Fig. 15). The cracks were first observed in B1, U1 and U2 near the start of phases of accelerated heave (B1) or progressive heave (U1 and U2) (Fig. 5). Segregated ice was observed as lenses usually no thicker than a few millimetres (maximum = 10 mm) within many of the cracks. Pore ice was present in interstices within the chalk between the cracks, as indicated its shiny appearance while the blocks remained frozen. In addition, a single macrocrack was found across the whole block B4 between a depth of 200 and 270 mm, and had a few small offshoot cracks. Unlike the cracks described previously in frozen blocks, this crack was not observed until the block had thawed.

4. Discussion

Four processes, operating singly or in combination in the blocks are inferred from our observations of heave, settlement and fracture.

4.1. Thermal expansion and contraction

Thermal expansion and contraction caused heave and settlement of the driest blocks throughout the experiments and influenced the behaviour of the other blocks when little or no phase change occurred between liquid water and ice. Thermal strain accounts for the 'winter heave' and 'winter settlement' shown by B3 and B4 (Figs. 8A and 9A) and for most of the heave and settlement behaviour of U5 and U6 (Fig. 11B,C). Because the rock blocks were unconfined vertically upwards (and horizontally), in order to simulate the upper surface of a natural rock outcrop, thermal stresses caused these blocks to heave (expand) during warming phases and settle (contract) during cooling phases.

Similar directional strains have been monitored at the surface of a bedrock block of migmatite granite in southern Finland, which heaved vertically upward in summer and settled in winter, the movements strongly correlated with rock temperature **(**Lehmuskoski et al., 2006; Hokkanen et al., 2007). These authors found that the movement exceeded the expected thermal expansion effect by an order of magnitude, and they suggested a lever system related to thermal expansion of bedrock. More generally, thermal stresses may generate thermal fatigue and thermal shock in the outermost centimetres of rock and may constitute a significant cause of rock weathering, particularly in arid cold regions (Hall, 1999; Hall and Thorn, 2014).

4.2. Volumetric expansion

Volumetric expansion of pore water freezing in situ caused short bursts of early winter heave and early summer settlement in wet blocks B1 and B2 (Figs. 6A and 7A) and U1 and U2 (stages '1' and '4' in Fig. 10A,B). The bursts coincided with the start of freezing and thawing periods, when the upper millimetres of rock quickly froze or thawed, limiting migration of unfrozen water. Similar behaviour has been recorded in experiments with rapid freezing and thawing of small specimens of saturated tuff (Figs. 12 and 13 of Matsuoka, 1990), near-saturated tuffeau (Fig. 2 of Prick, 1995), and sandstone at 50% and

90% saturation ('stage III' in Fig. 4 of Jia et al., 2015). We suggest that limited water migration occurred in all these experiments but did not keep pace with rapid frost penetration.

In the present experiments, rapid heave and settlement attributed to volumetric expansion dominated the overall heave behaviour in the first 10 freeze-thaw cycles in the bidirectional freezing experiment (Figs. 5A,B, 6A and 7A), but in subsequent cycles they became less distinct. By contrast, rapid heave of stage 1 and, to a lesser degree, settlement of stage 4 (Fig. 10A,B) persisted through most of the 27 freeze-thaw cycles of the unidirectional freezing experiment (Fig. 5C). The fundamental difference relates to progressive accumulation of segregated ice in the upper layer of permafrost in the bidirectional experiment.

4.3. Ice segregation and rock fracture

Ice segregation is indicated by the formation of segregated ice within newly formed macrocracks and by heave during both thawing and freezing periods (Murton et al., 2006). In the bidirectional experiment segregated ice accumulated incrementally near the permafrost table (Figs. 12 and 14), whereas in the unidirectional experiment it grew and melted during each cycle in the upper third of the block (Figs. 13 and 15). Unlike the abrupt heave that we attribute to volumetric expansion at the start of freezing periods, heave resulting from ice segregation was sustained for longer periods of time and occurred during both thawing and freezing periods. Heave during thawing periods ('summer heave' in Figs. 6B, 6C, 7A and 7B) tended to be greatest during their middle to late stages, when temperatures in the active layers were more or less constant through time but declined with depth, driving unfrozen water down into cracks in the uppermost layer of permafrost. The same process causes summer frost heave by ice segregation in Arctic permafrost soil (Mackay, 1983). Summer heave passed, with a small inflection (Figs. 6B and 7B), into early winter heave, as upward freezing from the permafrost table (Fig. 3A) caused ice segregation in the lower part of the active layer, at the same time as the upper millimetres of the active layer heaved rapidly by volumetric expansion.

The influence of ice segregation on heave behaviour changed over time from subordinate to dominant in the two wettest blocks (B1 and B2) in the bidirectional experiment. In the first 10 freeze-thaw cycles, heave was dominated by bursts attributed to volumetric expansion, while smaller amounts of heave occurred gradually during some thawing periods, as illustrated for all four blocks in Fig. 5B, and particularly clearly for B2 during thawing period 5 (Fig. 7A 'summer heave'). We attribute this small amount of heave to the progressive accumulation of segregated ice, too small to be visible to the naked eye, in microcracks developing near the permafrost table. During thawing period 10 in B1 and thawing period 21 in B2, ice segregation began to dominate the heave behaviour, following the development of the first macrocrack observed. We infer that once microcracks merged to form macrocracks, ice segregation and resulting frost heave increased substantially, and started to dominate the heave behaviour. This represents the crossing of a threshold in heave behaviour. The onset of macrocracking and frost heave at the same time has also been measured, under a sustained temperature gradient, in Kimachi sandstone and Noboribetu soft rock by Nakamura et al. (2007). The orientation of macrocracks in the present experiment, dominantly horizontal to subhorizontal, was parallel to the freezing fronts and similar to crack patterns formed by ice segregation in Ohya tuff (Fig. 1 of Nakamura et al., 2014).

Segregated ice accumulated incrementally in the uppermost layer of artificial permafrost and episodically melted. Rates of accumulation after thawing period 10 in B1 range from 0.26 to 6.19 mm per thawing period (Table S1), similar to estimates of between 0.2 and 5.0 mm yr^{-1} for annual accumulation of aggradational ice (mostly segregated ice) in near-surface permafrost in wet frost-susceptible Arctic permafrost soil (Mackay and Burn, 2002; O'Neill and Burn, 2012). Accumulation of an ice-rich layer in rock (or soil) renders the near-surface permafrost sensitive to late-summer air

temperatures (or wet summer conditions), which can lead to rapid melt of the segregated ice closest to the rock surface and therefore settlement of the rock surface, as occurred for B1 during high air temperatures of thawing period 18 at the start of the European heatwave of summer 2003 (Fig. 5A). As air temperature varied from cycle to cycle so melt and settlement varied (Table S1), similar to natural inter-annual variability of heave and settlement of frost-susceptible Arctic permafrost soils.

The heave and settlement behaviour of the wettest blocks in both experiments is remarkably similar to that of frost-susceptible soil. The shape of the heave curves for blocks U1 and U2 resemble those monitored, during studies of solifluction under conditions of unidirectional freezing, in sandy silt soil in the laboratory (see 'Vire' soil in Fig. 4 of Harris et al., 1995) and a frost-susceptible soil in southern Norway (Fig. 8 of Harris et al., 2007). For example, all share a distinctive 'freezing shoulder' (stage 1 in Fig. 10A,B). Likewise, the heave curves, post-macrocracking, in blocks B1 and B2 of the bidirectional experiment closely resemble those measured in bidirectional freezing of soliflucting soil in the Caen cold rooms (Fig. 5 of Harris et al., 2008). All show a characteristic summer frost heave (Figs. 6B,C and 7B).

4.4. Freeze-thaw consolidation

Freeze-thaw consolidation may explain the progressive settlement of blocks subject to unidirectional freezing, which is clearest for blocks U1 and U2 during the first 15 cycles (Fig. 5C). The settlement is attributed to temperature-gradient-induced migration of unfrozen water (cryosuction) towards freezing sites, causing an increase in effective stress below the freezing front and consolidation of that part of the rock from which water was drawn out of (cf. Thomachot and Matsuoka, 2007). Such consolation can result from freeze-thaw cycling of saturated fine-grained soils (Chamberlain and Gow, 1979) and mine tailings (Dawson et al., 1999), where it causes a net decrease in the void ratio and an increase in permeability. The freeze-thaw behaviour of the chalk was qualitatively similar to that of frost-susceptible soil because not only did ice segregation occur (Section 4.3.) but vertical to subvertical cracks (Fig. 13D) developed that are similar to vertical shrinkage cracks formed by freezing of saturated fine-grained soils (Chamberlain and Gow, 1979; Arenson et al., 2008). Freeze-thaw consolidation also occurs in fine-grained soils in active layers, as reported in western Arctic Canada (Smith, 1985; Mackay and Burn, 2002). The apparent absence of freeze-thaw consolidation in the bidirectional freezing experiment may be because the volume subject to freeze-thaw cycles was about 50% smaller than that in the unidirectional experiment and because accumulation of segregated ice in the uppermost permafrost counteracted consolidation.

Freeze-thaw consolidation of the tuffeau probably resulted from emptying and closing of fine pores when unfrozen water, drawn by cryosuction, migrated from fine pores towards larger partially empty pores, where ice was forming (Prick, 1995; Prick et al., 1993). These authors, who examined the dilation behaviour of the same tuffeau lithology that we have used, concluded that very small pores (<0.05 μm in diameter) allow shrinkage by desiccation, permitting contraction of tuffeau with a saturation coefficient of 72% during freezing; conversely, filling of these tiny pores during thawing promoted dilation (heave). We note, however, that it is difficult to distinguish such consolidation during freezing of unsaturated tuffeau from thermal contraction, except when contraction occurs without a change in temperature. Evidence for migration of unfrozen water due to cryosuction in the present experiments is shown where the unfrozen water content dropped as the active layer froze, with the minimum value occurring in the centre of the active layer (150 mm depth) at day 113 (Fig. 3B), because water had migrated towards both the permafrost and the rock surface. Such dewatering at 150 mm depth, induced by bidirectional freezing of the active layer, characterised the late stages of the freezing periods and the early stages of the thawing periods in B1.

Freeze-thaw consolidation of U1 and U2 ended about half way through the unidirectional freezing experiment and was replaced by net heave that we attribute to developing networks of macrocracks.

Significantly, the first macrocracks were observed about the time when the net heave commenced (Fig. 5C). As the cracks grew in number and length, the rock dilated and heaved. The absence of macrocracks in blocks U3 to U6 is consistent with the absence of a net heave trend (Fig. 5C).

5. Conclusions

We draw the following conclusions from this experimental study:

1. The heave and settlement behaviour of the tuffeau is essentially the same as that of frost-susceptible soil, because their porosity and pore-size characteristics are similar and the tensile strength of the tuffeau is small (0.07 to 1.07 MPa; see Murton et al., 2000). The main difference is probably that cementation of the chalk (causing increased tensile strength) delayed the appearance of macrocracks and ice lenses (cf. Nakamura et al., 2007) for several freeze-thaw cycles, relative to fissuring and ice lensing during the first freeze-thaw cycle in most soils.

2. Thermal expansion and contraction controlled rock heave and settlement when little or no water-ice phase change was involved. Such thermal strain, however, was overshadowed in moist to saturated rock by (1) volumetric expansion, (2) ice segregation or (3) freeze-thaw consolidation.

3. Volumetric expansion of water freezing in situ caused bursts of heave as wet rock froze rapidly at the onset of freezing periods and was followed by rapid settlement at the onset of thawing periods, corresponding to the growth and melt of pore ice in the outermost millimetres of rock. In the bidirectional experiment, bursts of heave and settlement were clearest during the first several cycles before being overshadowed by heave due to ice segregation.

4. Ice segregation initially led to microcracking and gradual accumulation of segregated ice (too small to be visible to the naked eye) in the uppermost layer of permafrost, as indicated, in the early cycles of the bidirectional experiment, by gradual heave of the rock surface during thawing periods. When the microcracks joined to form macrocracks, a threshold was passed, after which the magnitude of heave (and settlement) increased by an order of magnitude. Ice segregation led to sustained periods of heave during the middle to late stages of thawing periods (‘summer heave’) as water migrated down into the upper layer of permafrost, driven by gravity and cryosuction, and visible segregated ice accumulated incrementally in macrocracks. This accumulation left the near-surface permafrost vulnerable to melt and settlement during unusually warm summer conditions, producing substantial variability of heave and settlement between freeze-thaw cycles.

5. Freeze-thaw consolidation resulted when unfrozen water, driven by cryosuction, migrated from the finest pores towards freezing sites and caused an increase in effective stress below the freezing front and consolidation of that part of the rock from which water was drawn out of. Such consolidation caused net settlement of the surface of the two wettest blocks subject to unidirectional freezing, until a developing macrocrack network led to net dilation and heave.

The wider implications of this study to field studies of frost-susceptible bedrock are as follows:

6. Continuous monitoring of bedrock permafrost heave and settlement with relatively inexpensive and robust displacement transducers may indicate the change from subsurface microcracking to macrocracking. This may be particularly useful in monitoring mountain rock walls that contain pre-existing microcracks between joints.

7. Ice segregation and bedrock fracture are favoured in wet parts of the environment, such as depressions, river valleys, and coasts, as inferred previously by Matsuoka (2008).

8. Fractured bedrock (regolith) formed by ice segregation in the upper layers of permafrost beneath natural hillslopes or artificial slopes is liable to heave and settle seasonally or episodically, gradually moving downslope by solifluction (frost creep and gelifluction) and/or creep of ice-rich permafrost. This may have contributed to the downslope deflection of brecciated slates and shales commonly observed in areas of past permafrost, such as southwest England (Murton and Ballantyne, 2016) and northwest France.

Acknowledgements

This study was funded by the UK Natural Environmental Research Council (grant NER/A/S/2001/00506). We thank T. Cane, G. Guillemet, B. Jackson and P. Simmons for providing technical support for the experiments. Two anonymous reviewers and Editor-in-Chief Dr Takashi Oguchi are thanked for their valuable comments, which helped to improve the manuscript.

References

Arenson, L.U., Azmatch, T.F., Sego, D.C., Biggar, K.W., 2008. A new hypothesis on ice lens formation in frost-susceptible soils. In: Kane, D.L., Hinkel, K.M. (Eds.), Proceedings of the Ninth International Conference on Permafrost, June 29‑July 3, 2008, Institute of Northern Engineering, University of Alaska Fairbanks, Fairbanks, AK, Vol. 1, pp. 59–64.

Burn, C.R., 1984. Comments on “Frost-heaved bedrock features: a valuable permafrost indicator” by Jean-Claude Dionne. Géographie physique et Quaternaire 38, 205–207. DOI: 10.7202/032554ar

Chamberlain, E.J., Gow, A.J., 1979. Effect of freezing and thawing on the permeability and structure of soils. Engineering Geology 13, 73–92. DOI:10.1016/0013-7952(79)90022-X

Dawson, R.F., Sego, D.C., Pollock, G.W., 1999. Freeze-thaw dewatering of oil sands fine tails. Canadian Geotechnical Journal 36, 587–598. DOI: 10.1139/t99-028

Dionne, J-C., 1983. Frost-heaved bedrock features: a valuable permafrost indicator. Géographie physique et Quaternaire 37, 241–251.

Dredge, L.A., 1992. Breakup of limestone bedrock by frost shattering and chemical weathering, eastern Canadian Arctic. Arctic and Alpine Research 24, 314–323. DOI: 10.2307/1551286

Dyke, L.D., 1984. Frost heaving of bedrock in permafrost regions. Bulletin of the Association of Engineering Geologists 21, 389–405. DOI: 10.2113/gseegeosci.xxi.4.389

Gruber, S., Haeberli, W., 2007. Permafrost in steep bedrock slopes and its temperature-related destabilization following climate change. Journal of Geophysical Research 112: F02S18. DOI:10.1029/2006JF000547.

Hall, K., 1999. The role of thermal stress fatigue in the breakdown of rock in cold regions. Geomorphology 31, 47–63. DOI:10.1016/S0169-555X(99)00072-0

Hall K., Thorn, C.E., 2014. Thermal fatigue and thermal shock in bedrock: an attempt to unravel the geomorphic processes and products. Geomorphology 206, 1–13. DOI:10.1016/j.geomorph.2013.09.022

Harris, C., Davies, M.C.R., Coutard, J-P., 1995. Laboratory simulation of periglacial solifluction: significance of porewater pressures, moisture contents and undrained shear strength during soil thawing. Permafrost and Periglacial Processes 6, 293–311. DOI: 10.1002/ppp.3430060403

Harris, C., Luetschg, M., Davies, M.C.R., Smith, F., Christiansen, H.H., Isaksen, K., 2007. Field instrumentation for real-time monitoring of periglacial solifluction. Permafrost and Periglacial Processes 18, 205–114. DOI: 10.1002/ppp.573

Harris, C., Kern-Luetschg, M., Murton, J.B., Font., M., Davies, M., Smith, F., 2008. Solifluction processes on permafrost and non-permafrost slopes: results of a large scale laboratory simulation. Permafrost and Periglacial Processes 19, 359–378. DOI: 10.1002/ppp.630

Hokkanen, T., Lehmuskoski, P., Kaukolinna, J., 2007. Seasonally moving bedrock block at Metsähovi, Finland. American Geophysical Union, Fall Meeting 2007, abstract #G43B-1203.

Hutchinson, J.N., 1991. Periglacial slope processes. In: Forster, A., Culshaw, M.G., Cripps, J.C., Little, J.A., Moon, C.F. (Eds.), Quaternary Engineering Geology. Geological Society, London, Engineering Geology Special Publications, 7, pp. 283–331.

Jia, H., Xiang, W., Krautblatter, M., 2015. Quantifying rock fatigue and decreasing compressive and tensile strength after repeated freeze-thaw cycles. Permafrost and Periglacial Processes 26, 368–377. DOI: 10.1002/ppp.1857

Kitagawa, S., Kawakami, Y., 1984. Deformation of tunnels by ground freezing. Journal of the Japan Society of Engineering Geology 25-2, 59–65.

Lehmuskoski, P., Rouhiainen, P., Saaranen, V., Takalo, M., Virtanen, H., 2006. Seasonal change of the bedrock elevation at the Metsähovi Levelling Test Field. Nordic Journal of Geodesy 3, 58–68.

Mackay, J.R., 1983. Downward water movement into frozen ground, western arctic coast, Canada. Canadian Journal of Earth Sciences 20, 120–134. DOI: 10.1139/e83-012

Mackay, J.R., Burn, C.R., 2002. The first 20 years (1978–1979 to 1998–1999) of active-layer development, Illisarvik experimental drained lake site, western Arctic Coast. Canadian Journal of Earth Sciences 39, 1657–1674. DOI: 10.1139/e02-068

Matsuoka, N., 1990. Mechanics of rock breakdown by frost action: an experimental approach. Cold Regions Science and Technology 17, 253–270. DOI:10.1016/S0165-232X(05)80005-9

Matsuoka, N., 2001. Direct observation of frost wedging in alpine bedrock. Earth Surface Processes and Landforms 26, 604–614. DOI: 10.1002/esp.208

Matsuoka, N., 2008. Frost weathering and rockwall erosion in the southeastern Swiss Alps: long-term (1994–2006) observations. Geomorphology 99, 353–368. DOI:10.1016/j.geomorph.2007.11.013

Murton, J.B., Ballantyne, C.K., (2016, in press). Periglacial and permafrost ground models for Great Britain. In: Griffiths, J., Martin, C. (Eds.), Engineering Geology and Geomorphology of Glaciated and Periglaciated Terrains, Geological Society, London, Engineering Group Special Publication.

Murton, J.B., Coutard, J-P., Ozouf, J-C., Lautridou, J-P., Robinson, D.A., Williams, R.B.G., Guillemet, G., Simmons, P., 2000. Experimental design for a pilot study on bedrock weathering near the permafrost table. Earth Surface Processes and Landforms 25, 1281–1294. DOI: 10.1002/1096-9837(200011)25:12<1281::AID-ESP137>3.0.CO;2-U

Murton, J.B., Coutard, J-P., Ozouf, J-C., Lautridou, J-P., Robinson, D.A., Williams, R.B.G., 2001. Physical modelling of bedrock brecciation by ice segregation in permafrost. Permafrost and Periglacial Processes 12, 255–266. DOI: 10.1002/ppp.390

Murton, J.B., Peterson, R., Ozouf, J-C., 2006. Bedrock fracture by ice segregation in cold regions. Science 314, 1127–1129. DOI:10.1126/science.1132127

Nakamura, D., Goto, T., Mori, N., Suzuki, T., Hiramatsu, M., 2007. Basic study on frost susceptibility of rock – comparing the physical characteristics of rock. In: The Eighth International Symposium on Cold Region Development. Finnish Association of Civil Engineers RIL, Tampere, Finland.

Nakamura, D., Kawaguchi, T., Goto, T., Yamashita, S., Ito, Y., Yamasaki, S., 2014. Measurement of suction pressure generated in the process of frost heaving in rock. In: Eighth Asian Rock Mechanics Symposium, 14–16 October 2014, Sapporo, Japan.

O'Neill, H.B., Burn, C.R., 2012. Physical and temporal factors controlling the development of near-surface ground ice at Illisarvik, western Arctic coast, Canada. Canadian Journal of Earth Sciences 49, 1096–1110. DOI:10.1139/E2012-043

Prick, A., 1995. Dilatometrical behaviour of porous calcareous rock samples subjected to freeze-thaw cycles. Catena, 25, 7–20. DOI:10.1016/0341-8162(94)00038-G

Prick, A., Pissart, A., Ozouf, J-C., 1993. Variations dilatométriques de cylindres de roches calcaires subissant des cycles de gel–dégel. Permafrost and Periglacial Processes 4, 1–15. DOI: 10.1002/ppp.3430040102

Schär, C., Vidale, P.L., Lüthi, D., Frei, C., Häberli, C., Liniger, M.A., Appenzeller, C., 2004. The role of increasing temperature variability in European summer heatwaves. Nature 427, 332–336. DOI:10.1038/nature02300

Smith, M.W., 1985. Observations on soil freezing and frost heaving at Inuvik, Northwest Territories, Canada. Canadian Journal of Earth Sciences 22, 283–290. DOI: 10.1139/e85-024

Smith, T., Milne, D., Hawkes, C., 2007. Case study review of rock mass response to artificial ground freezing. In: Proceedings of the 1st Canada-US Rock Mechanics Symposium, Vancouver, Canada, 2007, pp. 191–198.

Thomachot, C., Matsuoka, N., 2007. Dilation of building materials submitted to frost action. In: Přikyrl, R., Smith, B.J. (Eds.), Building Stone Decay: From Diagnosis to Conservation. Geological Society, London, Special Publications, 271, pp. 167–177.

Wegmann, M., Gudmundsson, G.H., 1999. Thermally induced temporal strain variations in rock walls observed at subzero temperatures. In: Hutter, K., Wang, Y., Beer, H. (Eds.), Advances in Cold-Region Thermal Engineering and Sciences. Springer, Berlin, pp. 511–518.

Tables

Table 1. Freezing regime, water supply, mean volumetric unfrozen water content (θ_u) and per cent saturation during freezing and thawing periods

Freezing regime	**Block**	**Water supply**	θ_{ut} **(%)**[b]	**% sat.** [c]	θ_{uf} **(%)**[d]	**% sat.** [c]
Bidirectional (active layer above permafrost)	B1	Water table at base during initial permafrost aggradation; thereafter surface sprinkling	41±6 AL 17±4 P	86±11 AL 34±9 P	14±2	29±5
	B2	Surface [a]	35±2 AL 17±6 P	72±5 AL 35±12 P	13±1	27±3
	B3	Surface [a]	24±1 AL 15±4 P	49±2 AL 31±9 P	12±1	24±3
	B4	None	8±2 AL 12±1 P	18±4 AL 25±2 P	8±3	17±5
Unidirectional (seasonal frost)	U1	Water table at base; water sprinkled onto surface	45±4	93±8	24±10	49±20
	U2	As above	43±4	90±8	20±5	42±10
	U3	Surface [a]	32±4	66±8	16±2	32±4
	U4	Closed system (block sealed in polythene)	35±5	73±8	17±1	35±3
	U5	Surface [a]	22±2	47±3	12±1	24±3
	U6	None	6±1	12±1	4±0	8±1

[a] Water sprinkled onto top of block during thawing periods.

[b] ϑ_{ut} = Mean volumetric unfrozen water content (%) at end of thawing periods (determined for whole block in U1–U6, and subdivided into active layer (AL) and permafrost (P) for B1–B4). *n* = 21 for B1–B4; *n* = 26 for U1–U6 (missing data for thawing period 26).

[c] % saturation = ϑ_{ut} / water porosity measured under vacuum; or ϑ_{uf} / water porosity measured under vacuum.

[d] ϑ_{uf} = Mean volumetric unfrozen water content (%) at end of freezing periods (determined for whole block). *n* = 17 for B1–B4 (missing data for freezing periods 11, 16, 18 and 19); *n* = 21 for U1–U6 (missing data for freezing periods 5, 13, 21, 22, and 26).

'±' measurements given as mean value of standard deviation for each freezing period and thawing period.

Table 2 Matrix of correlation coefficients (Pearson's *r*) between *ALT* versus air temperature and water content

		Max. air temp.	Mean air temp.	Vol. unfrozen water content in active layer at end of thawing cycles (θ_{ut})
ALT	B1 (wettest)	0.69 [a]	0.46 [c]	-0.51 [c]
	B2	0.66 [b]	0.44 [c]	0.44 [c]
	B3	0.73 [a]	0.64 [b]	0.43 [ns]
	B4 (driest)	0.87 [a]	0.72 [a]	0.64 [b]

[a] *p*-value (two-tailed) < 0.000

[b] *p*-value (two-tailed) < 0.00

[c] *p*-value (two-tailed) < 0.05

[ns] Not significant at 0.05 level

Figures

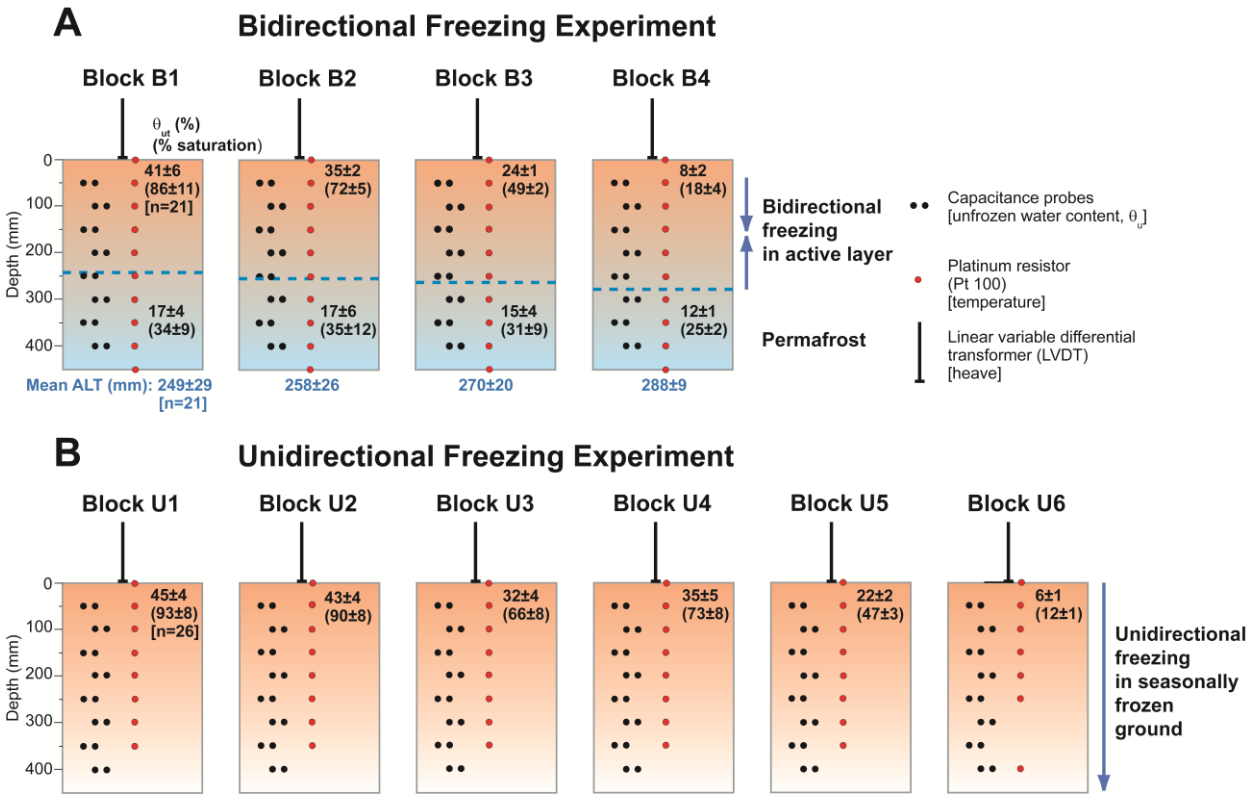

Fig. 1. Schematic diagram of freezing regimes, location of sensors and water contents for the bidirectional freezing experiment (A) and unidirectional freezing experiment (B). Values of mean volumetric water content are for the end of freezing periods (ϑ_{uf}) and the end of thawing periods (ϑ_{ut}) (± mean value of standard deviation per cycle). Mean values of active-layer thickness (*ALT*) (± 1 std dev.) are for the bidirectional freezing experiment. *ALT* for thawing period 18 is approximate due to missing data.

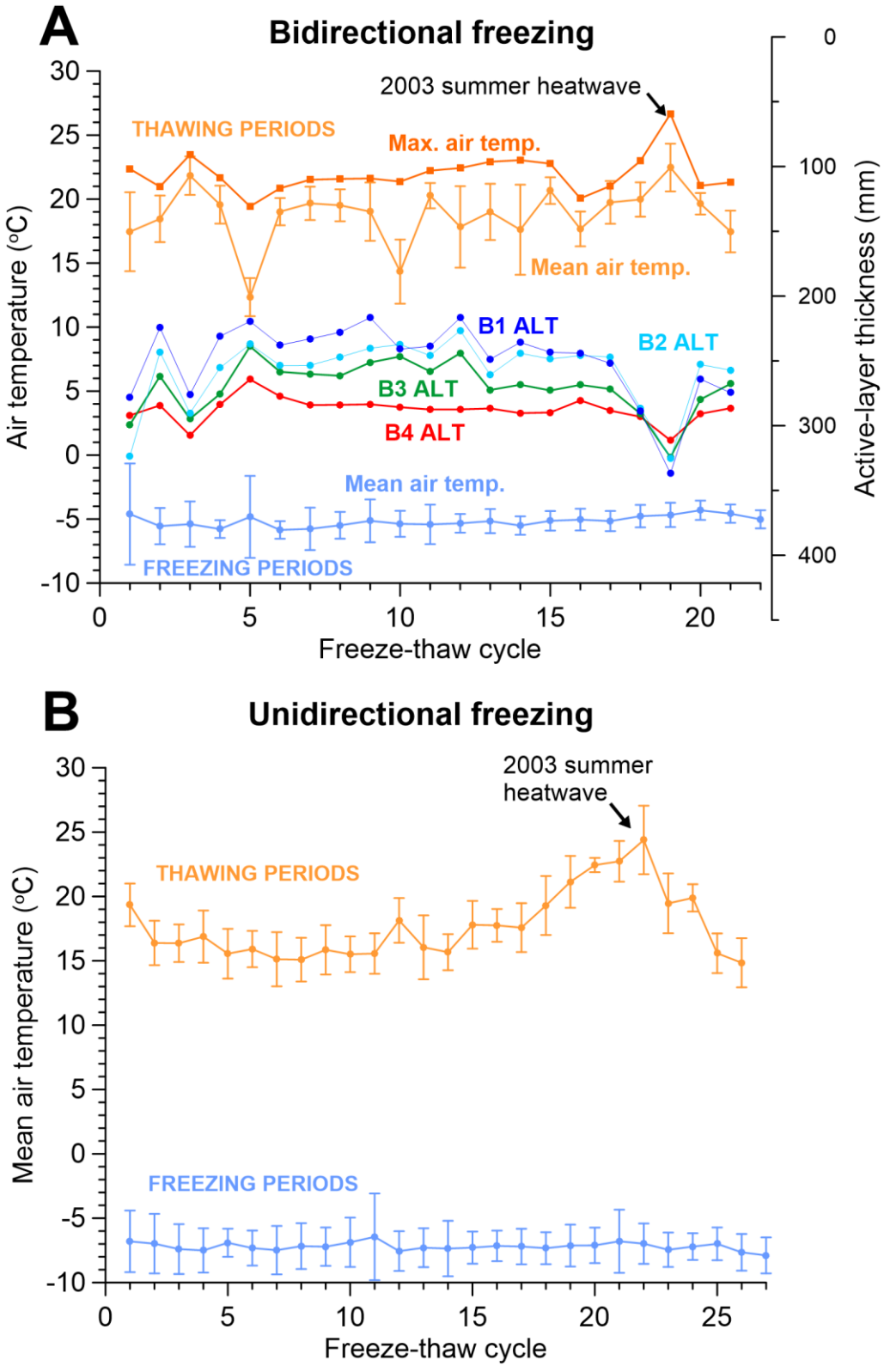

Fig. 2. Mean air temperature (± 1 std dev.) during the freezing and thawing periods of the bidirectional freezing experiment (A) and the unidirectional freezing experiment (B). Maximum air temperature during thawing periods and active-layer thickness (*ALT*) are also shown in (A).

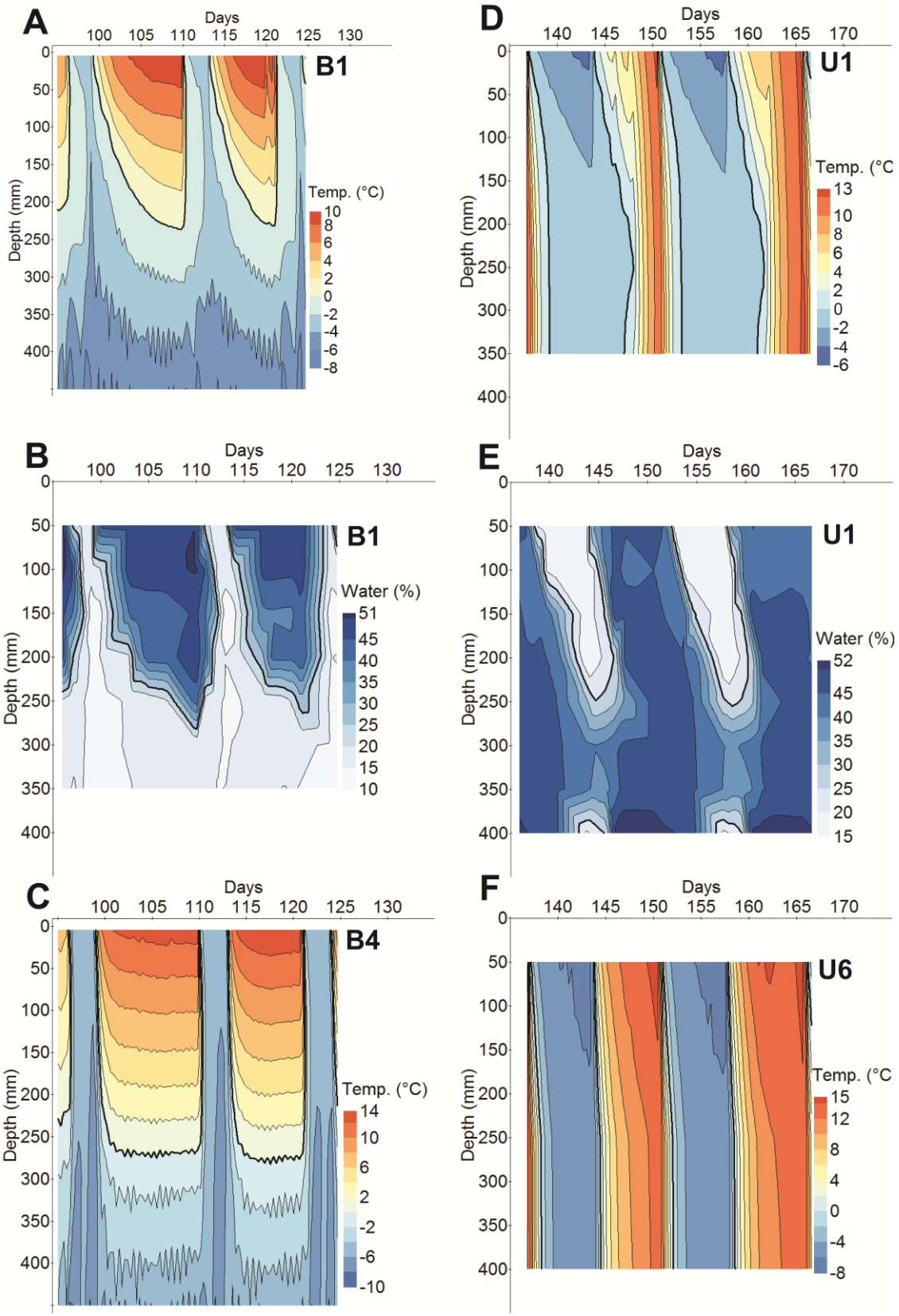

Fig. 3. Rock temperature and unfrozen volumetric water content time series between days 95 and 125 with depth for the wettest blocks (B1 and U1), compared with temperature between days 137 and 167 for the driest blocks (B4 and U6). Thick black lines in (A), (C), (D) and (F) indicate 0°C isotherm, and in (B) and (E) 25% water content. The upward attenuating spikes in (A) and (C) indicate upward cooling from the thermostatically controlled basal cooling plate.

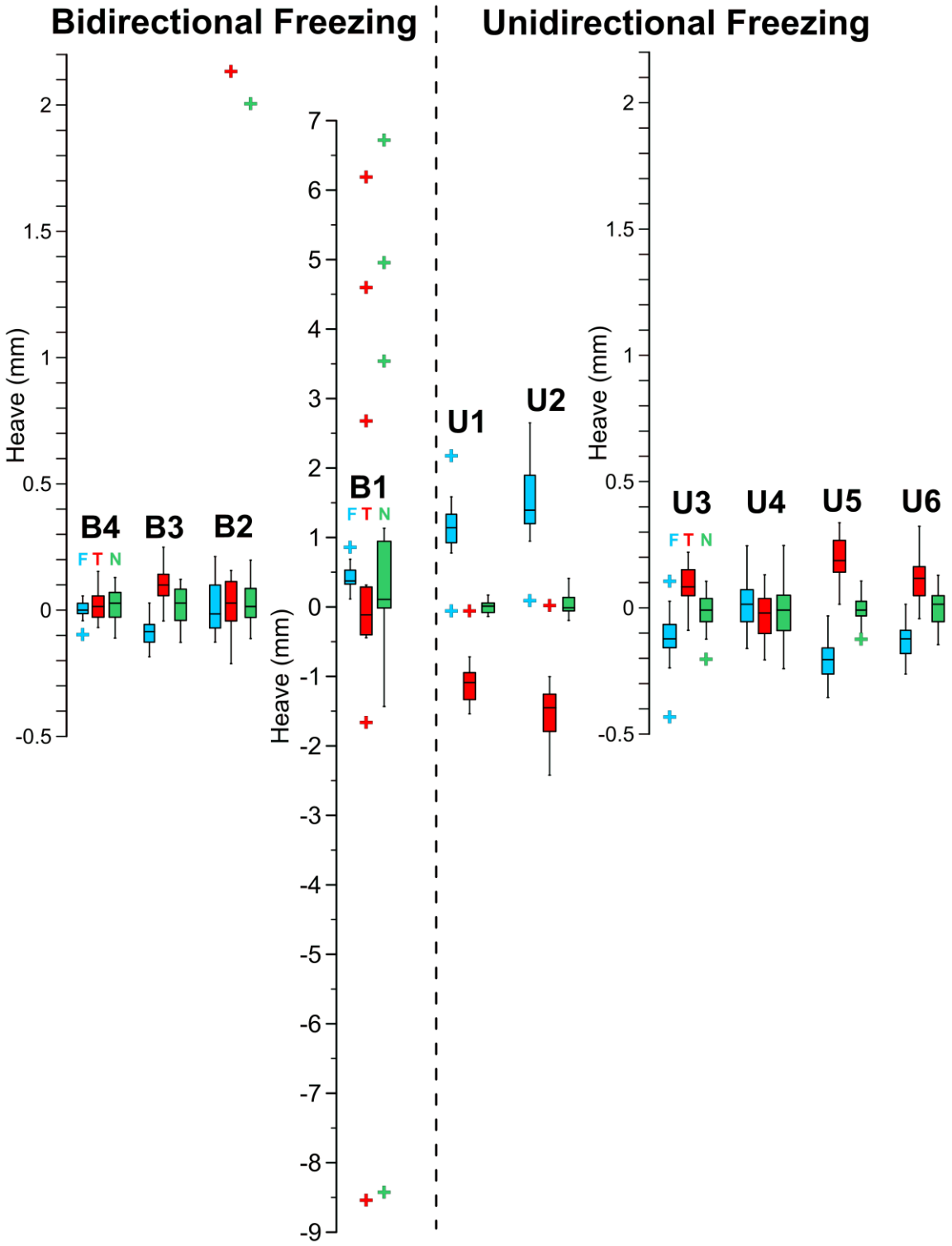

Fig. 4. Boxplots showing heave (positive values) and settlement (negative values) of the tops of blocks B1−B4 subjected to bidirectional freezing and blocks U1−U6 subjected to unidirectional freezing. 'F' above boxes (on left of each group of three boxes per block) indicates heave/settlement during freezing periods, 'T' above boxes (in middle) during thawing periods, and 'N' above boxes (on right) indicates net heave per cycle. Note extended scale on *y*-axis in middle of plot for the wettest blocks B1, U1 and U2. The boxes show the interquartile range, the horizontal line within the boxes is the median, and the whiskers extend to the highest and lowest values within 1.5 times the interquartile range. Outliers (crosses) are more than 1.5 times the interquartile range above the upper quartile or below the lower quartile. Vertical dashed line separates boxplots from the two experiments.

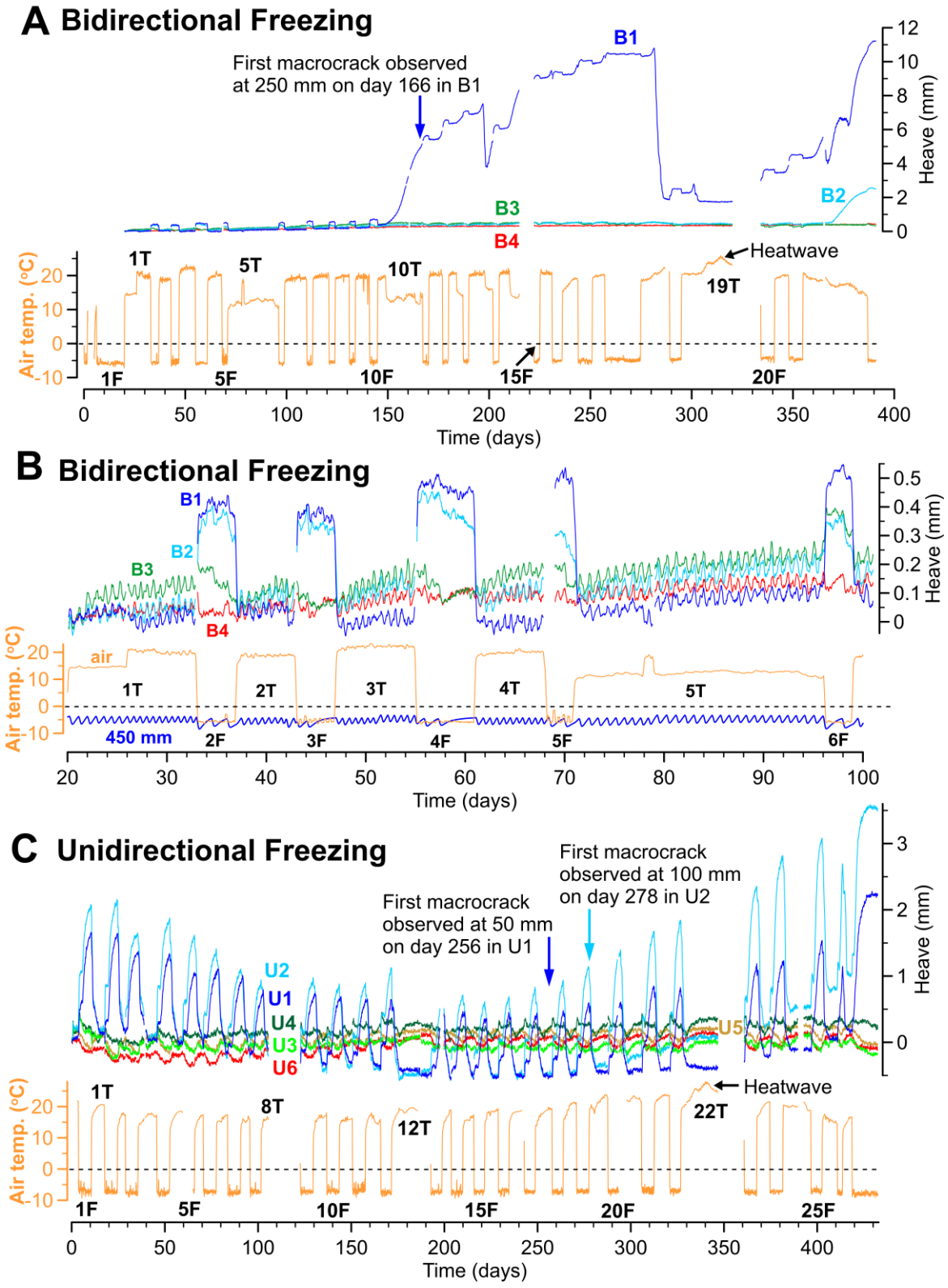

Fig. 5. Time series of heave and temperature. (A) Heave and air temperature during 21 cycles of bidirectional freezing of blocks B1−B4. ‘1F’ to ‘20F’ indicate freezing periods 1 to 20, and '1T' to '19T' indicate thawing periods. (B) Detailed heave behaviour between thawing period 1 (‘1T’) and freezing period 6 (‘6F’). The temperature at 450 mm depth is the mean value at the base of the four blocks. (C) Heave and air temperature during 26 cycles of unidirectional freezing of blocks U1−U6. Numbers below air temperature graph indicate freezing periods. Dashed black lines indicates 0°C. Note different vertical scales of heave in A to C.

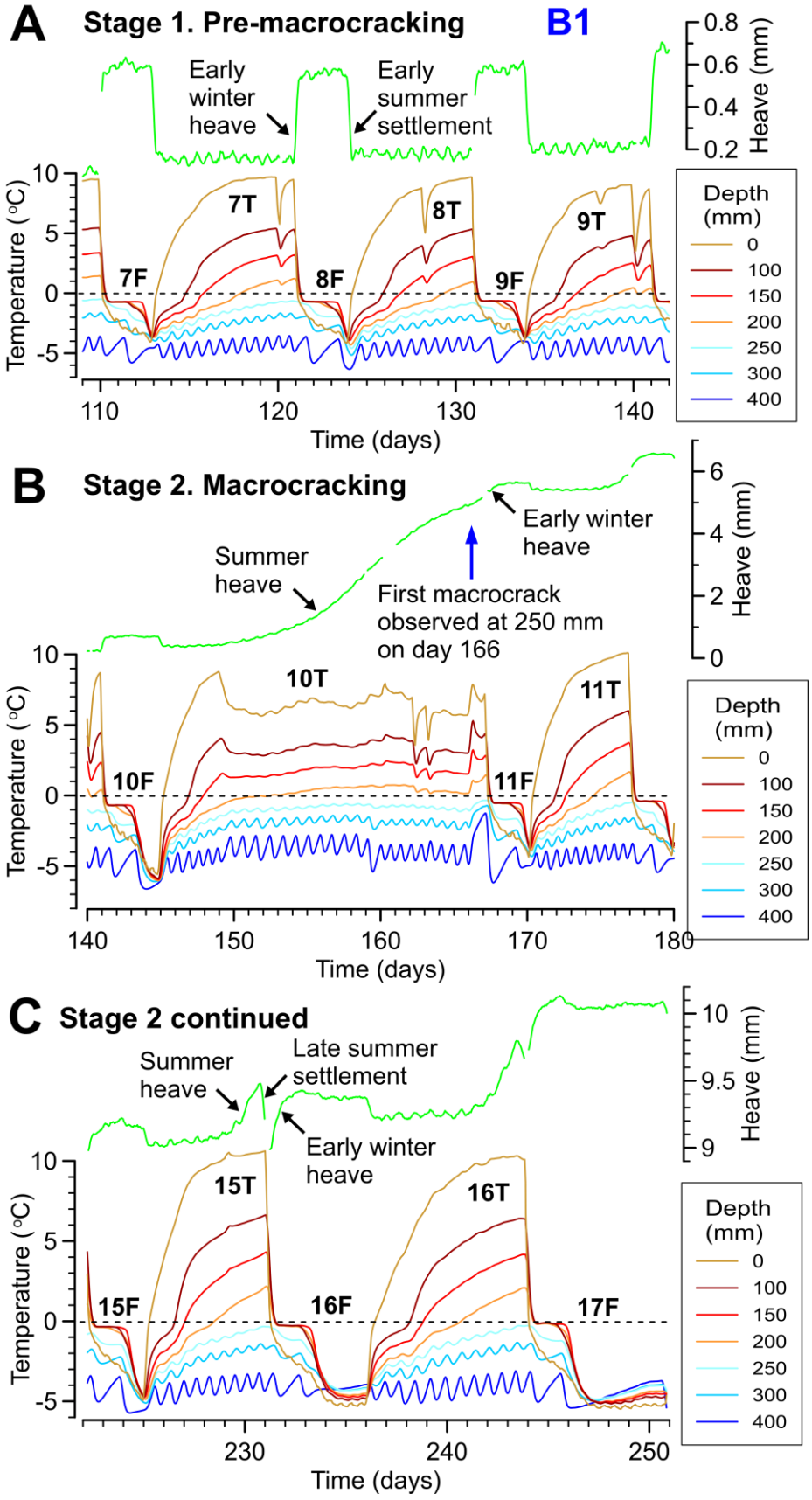

Fig. 6. Heave and rock temperature of block B1 during pre-macrocracking (A), macrocracking (B) and (C) stages. Freezing periods are numbered '7F' etc. and thawing periods are numbered '7T' etc. Note different vertical scales of heave in A to C.

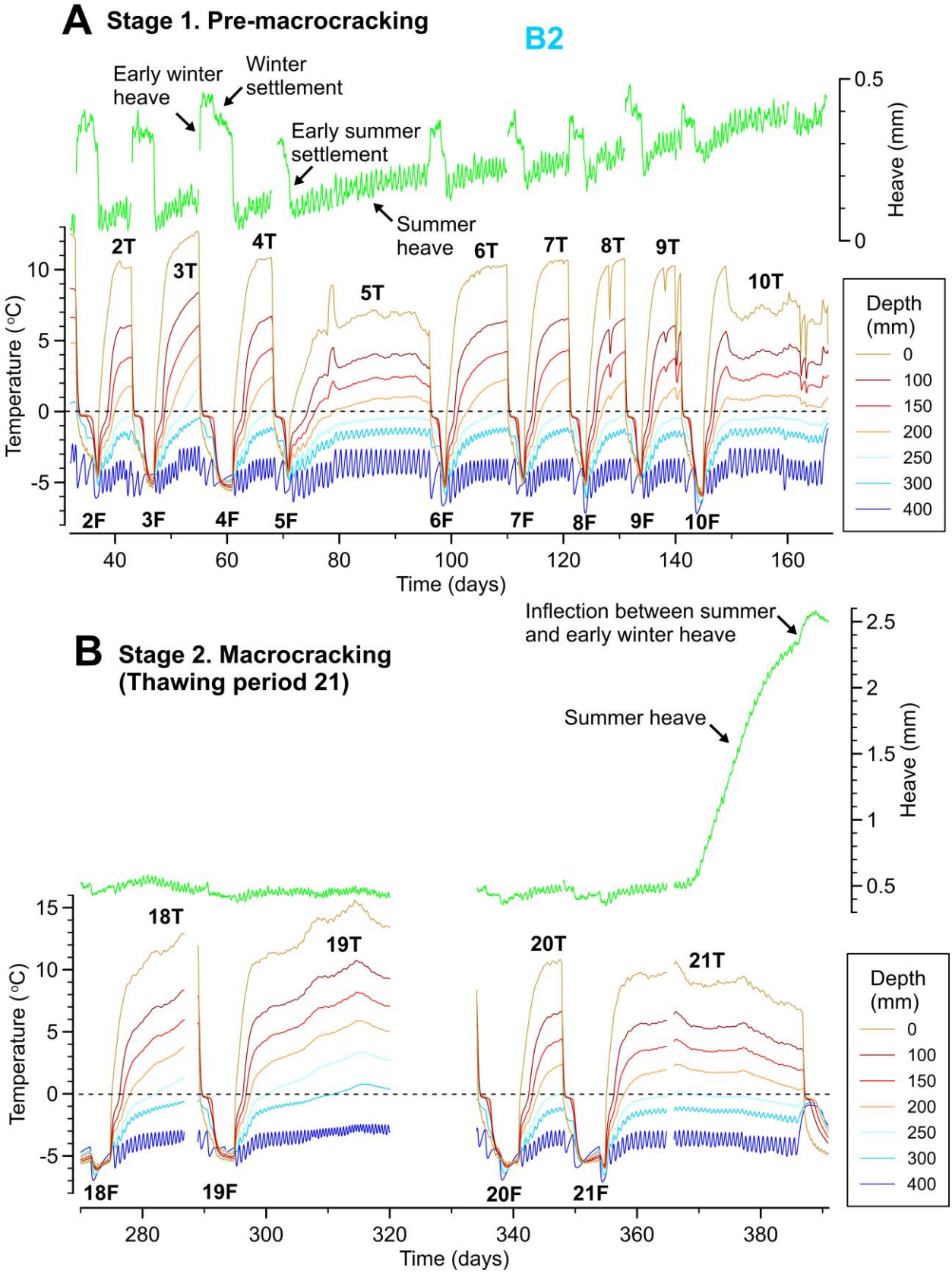

Fig. 7. Heave and rock temperature of block B2 during pre-macrocrack (A) and macrocrack (B) stages. Freezing periods are numbered '2F' etc.

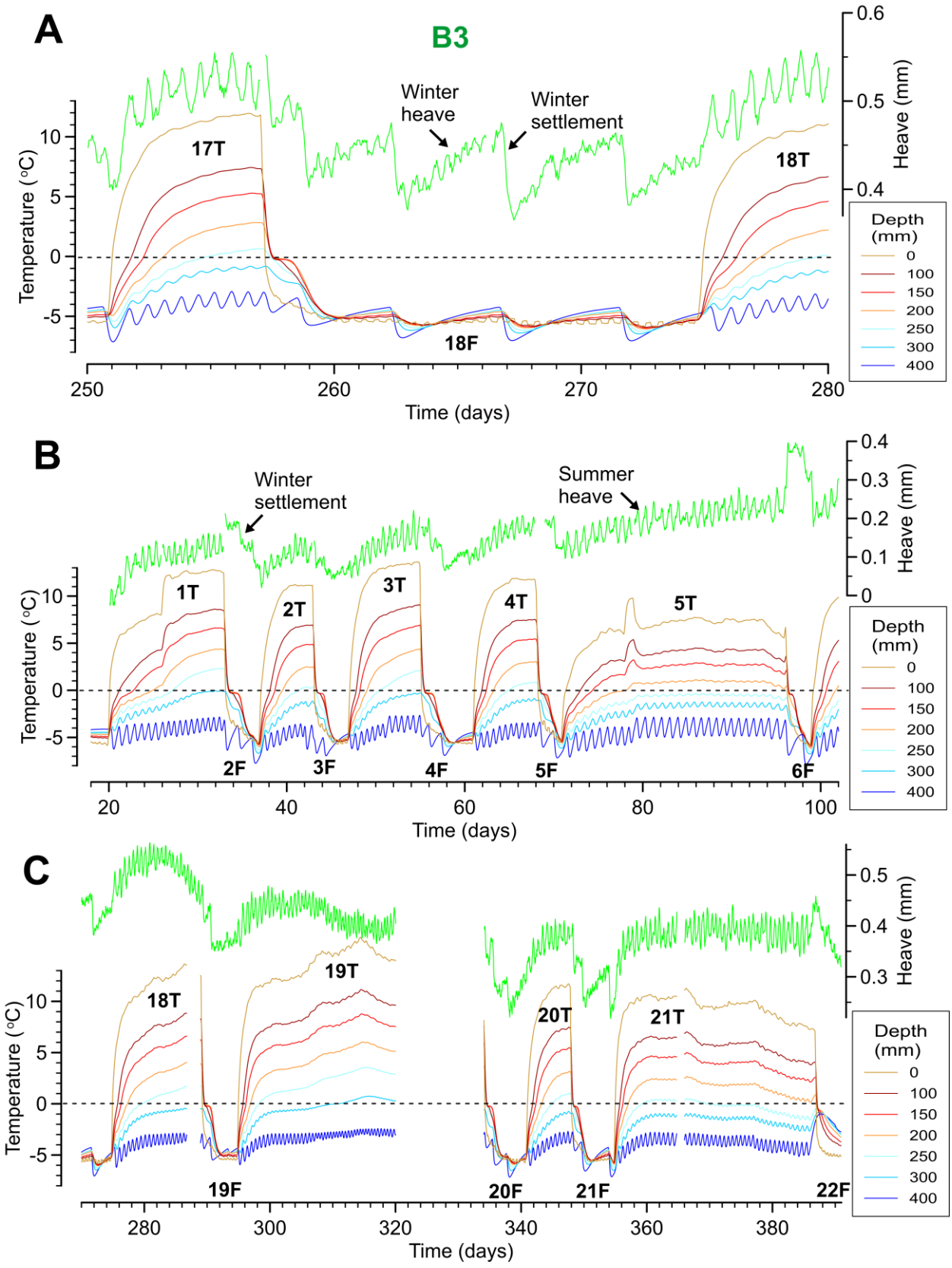

Fig. 8. Heave and rock temperature of block B3 during freezing period 18 (A), between thawing period 1 and freezing period 6 (B), and between thawing period 18 and freezing period 22 (C).

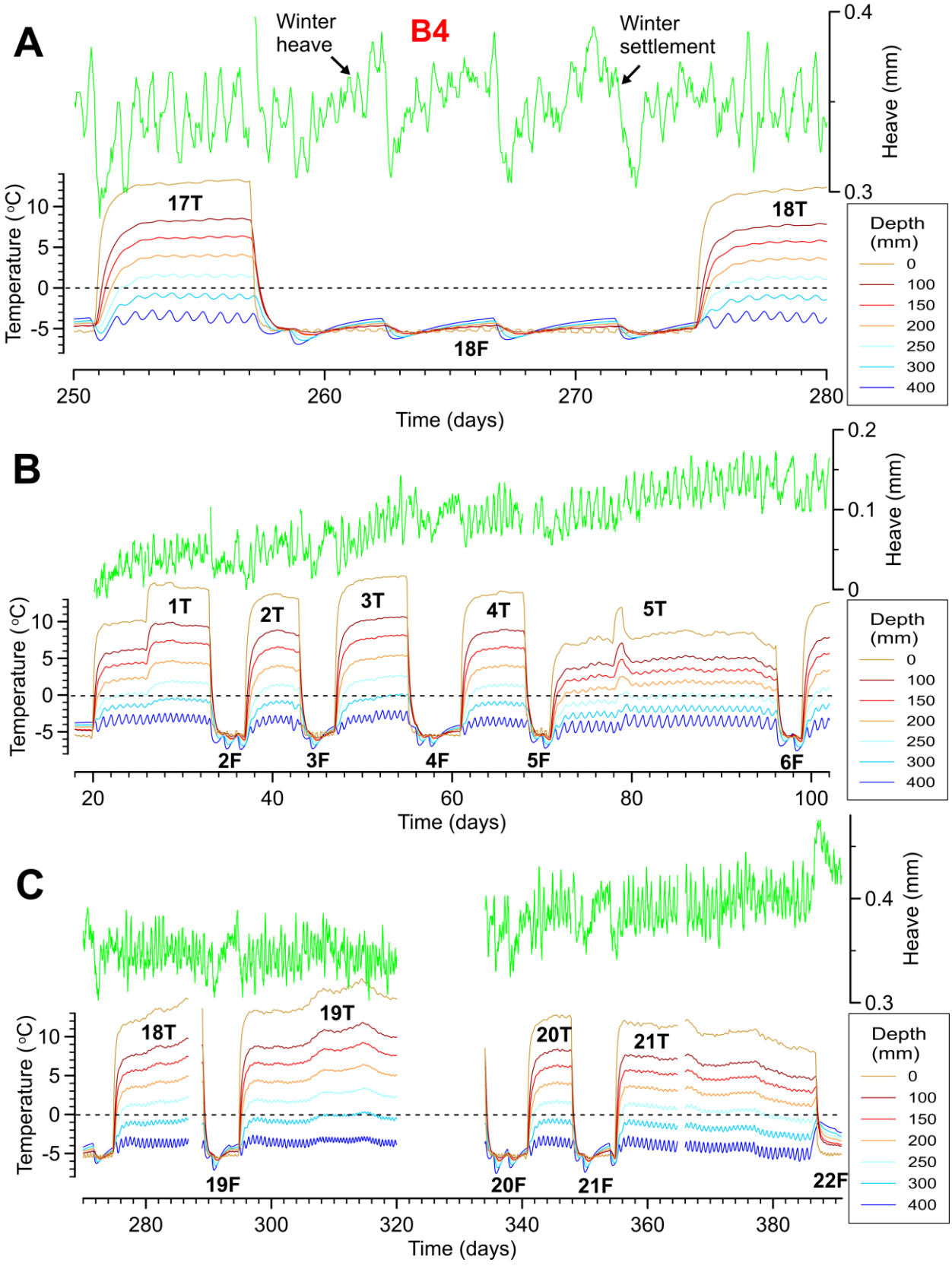

Fig. 9. Heave and rock temperature of block B4 during freezing period 18 (A), between thawing period 1 and freezing period 6 (B), and between thawing period 18 and freezing period 22 (C).

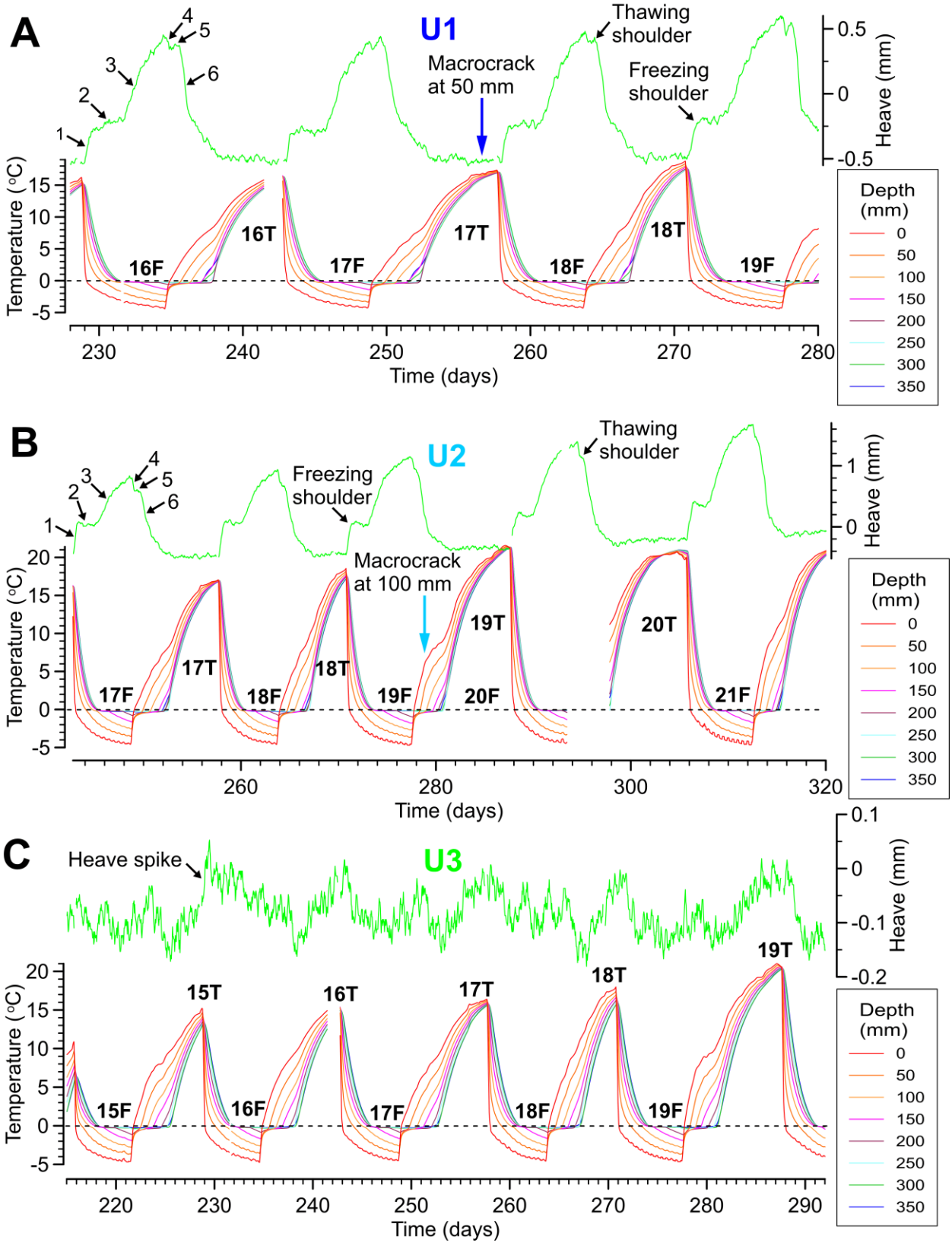

Fig. 10. Heave and rock temperature of blocks U1 (A), U2 (B) and U3 (C). Arrows on (A) and (B) mark the time when visible fractures where first observed in the blocks. 1, 2 and 3 on (A) and (B) indicate stages of heave, and 4, 5 and 6 indicate stages of settlement (see text).

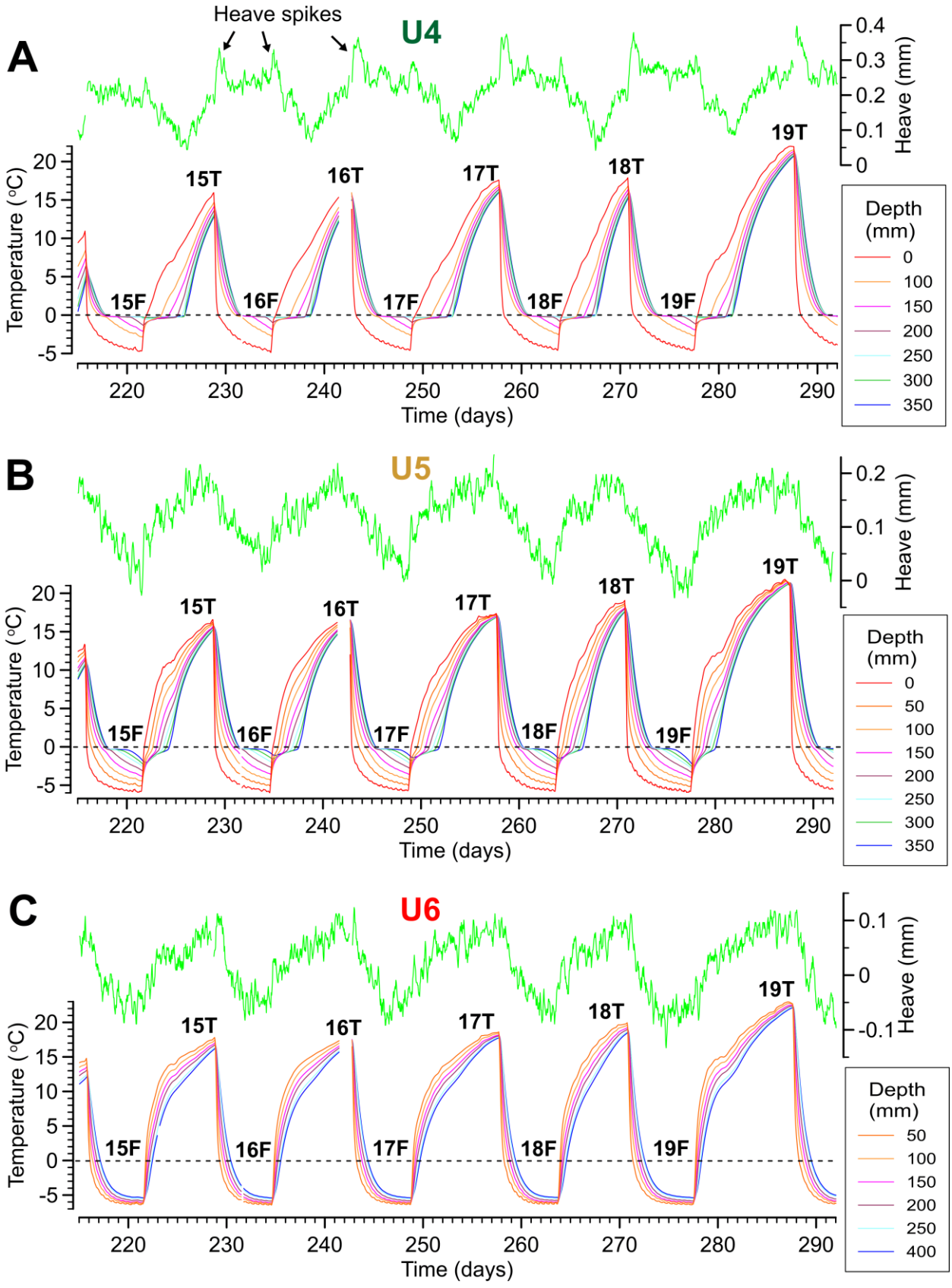

Fig. 11. Heave and rock temperature of blocks U4 (A), U5 (B) and U6 (C).

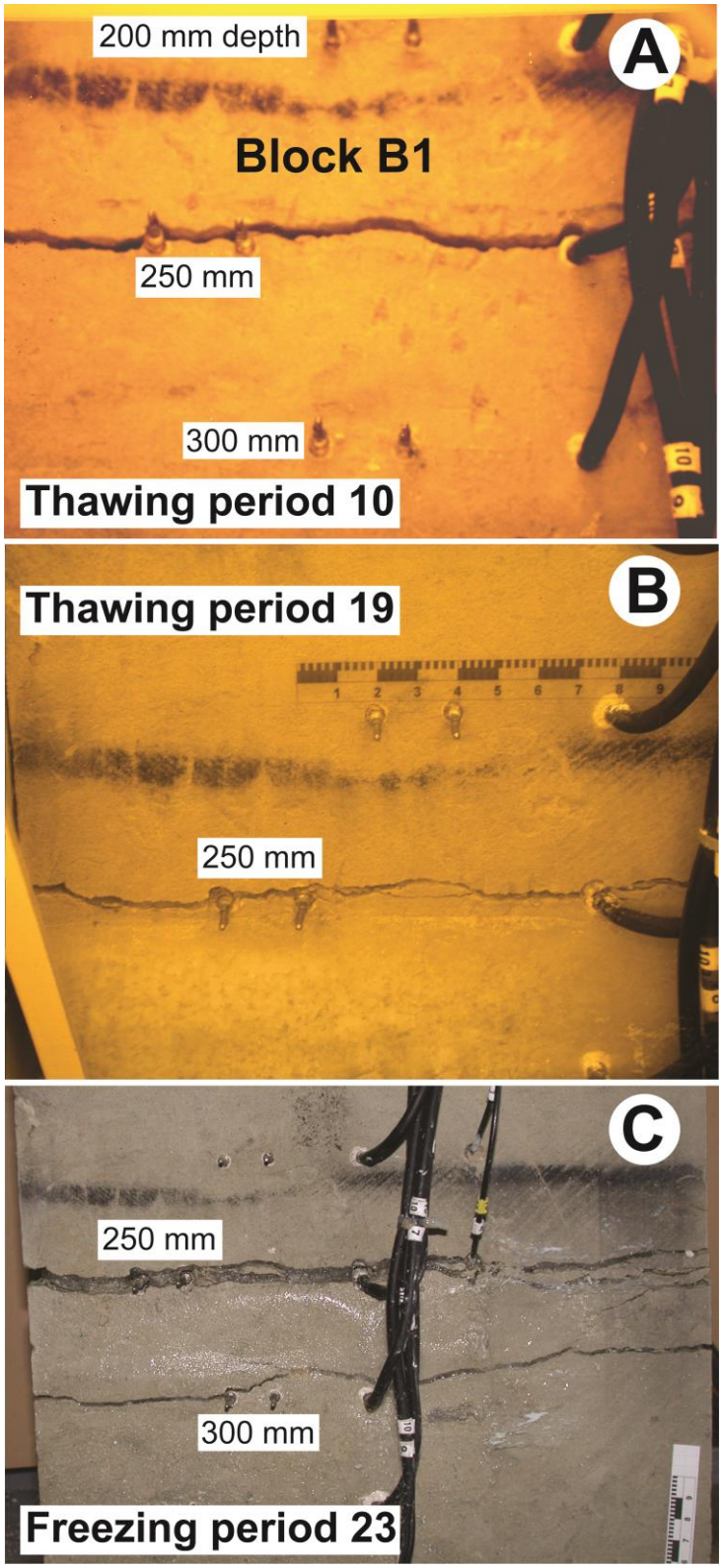

Fig. 12. Developing macrocracks network in block B1 during the bidirectional freezing experiment. The same vertical face was photographed during (A) thawing period 10, (B) thawing period 19 and (C) freezing period 23. Depths in (A) and (C) refer to depths of capacitance sensor rods below top of block. Note the horizontal macrocrack in (C) at a depth of about 300 mm which formed between thawing period 19 and freezing period 23. The segregated ice in the macrocrack at about 250 mm depth in (C) is about twice as thick as that shown in the same crack in (B) and must have developed mainly during thawing periods 21 and 22 (see heave curve in Fig. 5A). Note difference in vertical and horizontal scales, especially between B and C.

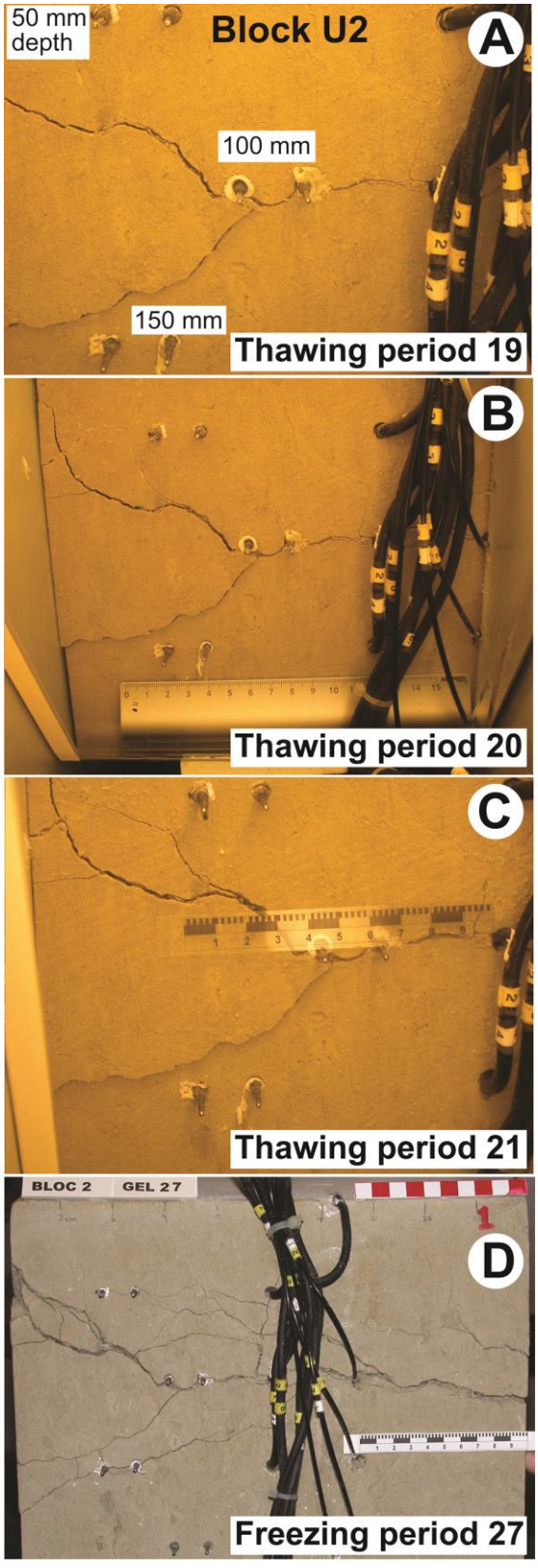

Fig. 13. Developing macrocrack network in block U2 during the unidirectional freezing experiment. The same vertical face was photographed during (A) thawing period 19, (B) thawing period 20, (C) thawing period 21 and (D) freezing period 27. Note occurrence of short vertical cracks linking horizontal to subhorizontal cracks in (D). Depths in (A) refer to depths of capacitance sensor rods below top of block. Note difference in vertical and horizontal scales, especially between C and D.

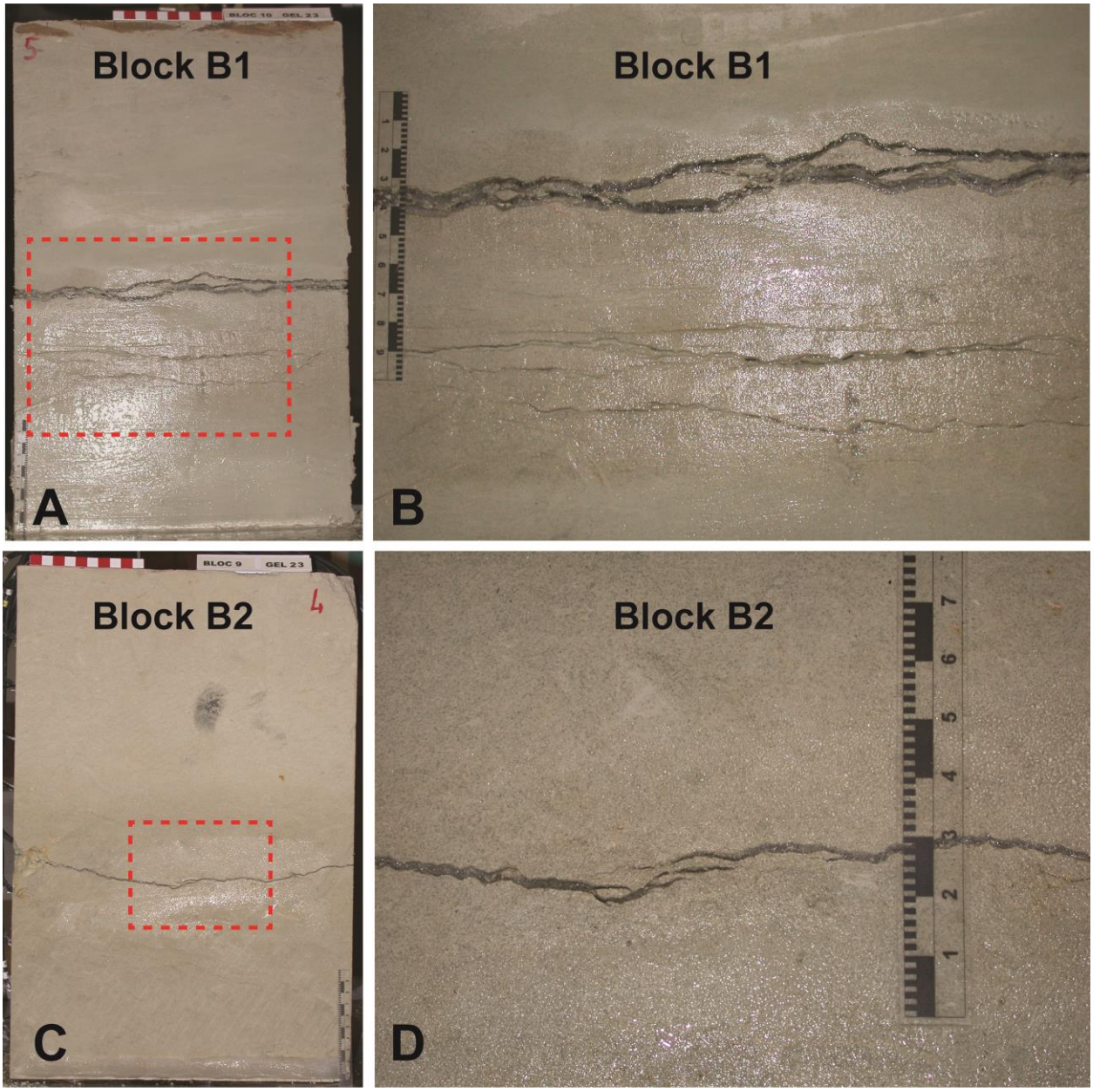

Fig. 14. Final macrocrack networks formed in blocks B1 (A and B) and B2 (C and D) at the end of freezing period 23 of the bidirectional freezing experiment. The blocks are frozen and the cracks are filled with segregated ice. Scales in centimetres and millimetres. (A) and (B) show a vertical section that was sawn through the frozen block, and represents the crack network in the inner part of the block. (C) and (D) show a vertical section through one of the original outer faces of the block.

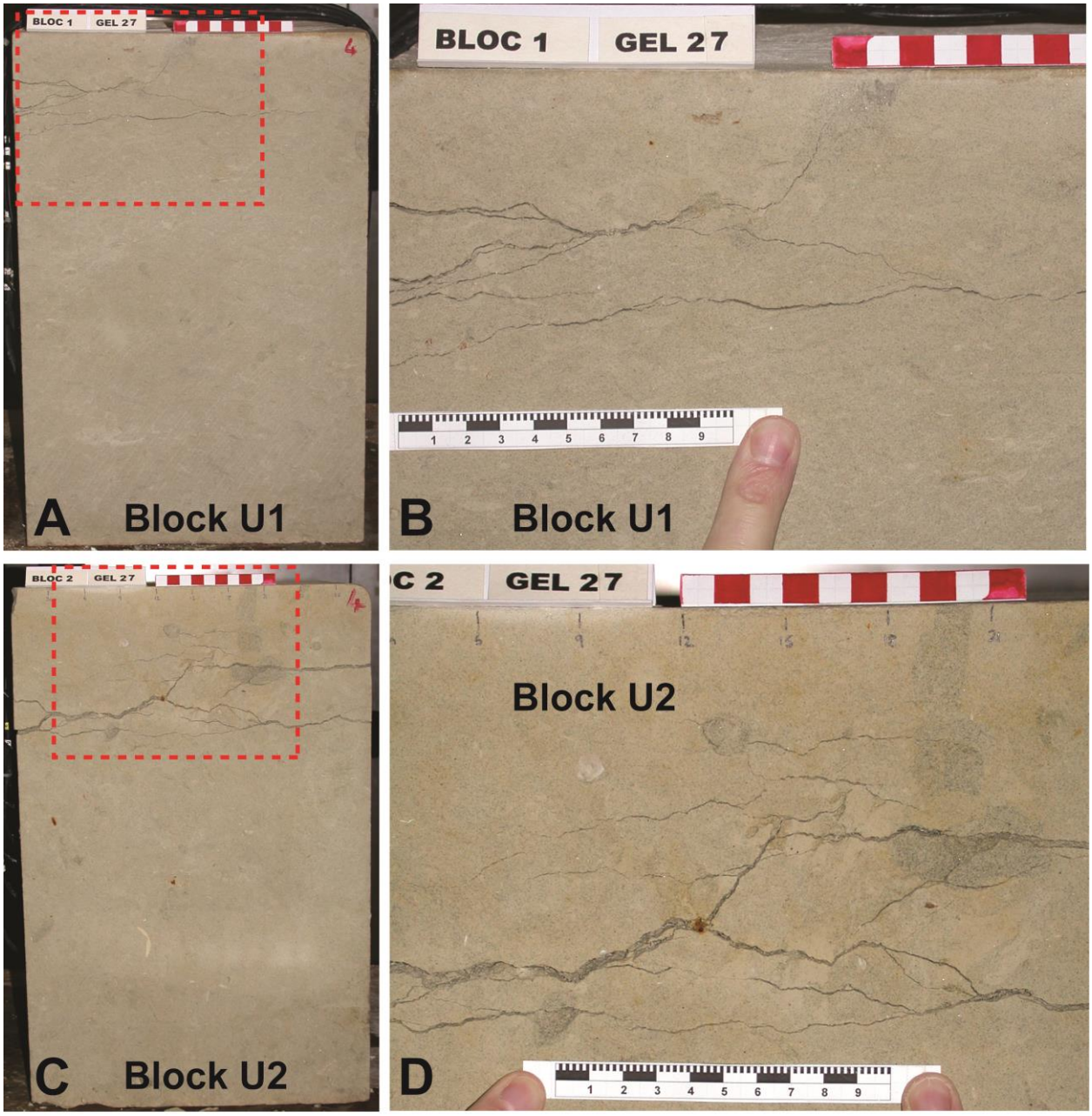

Fig. 15. Final macrocrack networks formed in blocks U1 (A and B) and U2 (C and D) at the end of freezing period 27, unidirectional freezing experiment. The blocks are frozen and the cracks are filled with segregated ice. Scales in centimetres and millimetres. (A) to (D) show vertical sections through one of the original outer faces of the blocks. The vertical face shown in (C) and (D) is perpendicular to the face shown in Fig. 13.

Supporting Information

Table S1 Heave and settlement of blocks B1 to B4 during freezing periods ('Freeze') and thawing periods ('Thaw') of the bidirectional freezing experiment

Table S2 Heave and settlement of blocks U1 to U6 during freezing periods ('Freeze') and thawing periods ('Thaw') of the unidirectional freezing experiment

SUPPORTING INFORMATION

Supporting Tables

Table S1 Heave and settlement of blocks B1 to B4 during freezing periods ('Freeze') and thawing periods ('Thaw') of the bidirectional freezing experiment

	B1 Heave (mm)			B2 Heave (mm)			B3 Heave (mm)			B4 Heave (mm)		
Cycle	**Freeze**	**Thaw**	**Net** [a]	**Freeze**	**Thaw**	**Net**	**Freeze**	**Thaw**	**Net**	**Freeze**	**Thaw**	**Net**
1		0.12			0.11			0.23			0.15	
2	0.22	-0.27	-0.06	0.14	-0.18	-0.04	-0.14	0.06	-0.09	-0.10	-0.01	-0.11
3	0.24	-0.20	0.04	0.21	-0.09	0.12	-0.09	0.17	0.08	0.01	0.07	0.08
4	0.33	-0.43	-0.10	0.11	-0.21	-0.10	-0.13	0.09	-0.04	-0.04	0.01	-0.03
5	0.50	-0.40	0.10	0.10	0.04	0.14	-0.06	0.13	0.07	0.00	0.03	0.03
6	0.37	-0.40	-0.03	0.01	-0.04	-0.03	0.03	0.06	0.09	-0.01	0.10	0.08
7	0.53	-0.44	0.09	0.10	-0.11	-0.01	-0.06	0.03	-0.03	-0.01	-0.03	-0.04
8	0.40	-0.42	-0.02	0.04	0.01	0.06	-0.03	0.13	0.10	0.01	0.01	0.03
9	0.37	-0.26	0.12	0.16	-0.07	0.09	-0.10	0.13	0.03	0.06	-0.03	0.03
10	0.36	4.60	4.96	-0.07	0.16	0.09	-0.13	0.25	0.12	0.00	0.13	0.13
11	0.42	0.26	0.67	-0.10	0.06	-0.04	-0.19	0.06	-0.13	-0.04	-0.04	-0.08
12	0.69	0.26	0.95	-0.07	0.14	0.07	-0.07	0.14	0.07	-0.01	0.06	0.04
13	0.23	-1.66	-1.43	-0.10	-0.02	-0.11	-0.13	0.07	-0.06	-0.01	-0.03	-0.04
14	0.86	2.68	3.54	0.06	0.14	0.20	-0.07	0.14	0.07	0.03	0.04	0.07
15	0.22	-0.11	0.10	-0.11	0.11	0.00	-0.14	0.10	-0.04	-0.04	0.01	-0.03
16	0.33	0.29	0.62	-0.06	0.03	-0.03	-0.04	0.07	0.03	0.03	-0.04	-0.01
17	0.37	0.30	0.67	-0.11	0.14	0.03	-0.10	0.10	0.00	0.03	0.03	0.06
18	0.12	-8.54	-8.43	-0.03	-0.04	-0.07	-0.06	0.03	-0.03	0.01	-0.01	0.00
19	0.60	0.32	0.92	-0.02	0.02	0.00	-0.09	-0.04	-0.13	0.06	-0.07	-0.01
20	0.86	0.27	1.13	-0.04	0.07	0.03	-0.07	0.10	0.03	0.03	0.00	0.03
21	0.53	6.19	6.72	-0.13	2.13	2.01	-0.13	0.21	0.09	0.00	0.08	0.08
22	0.57			-0.01			-0.02			-0.01		
Mean	0.43	0.10	0.53	0.00	0.11	0.12	-0.09	0.11	0.01	0.00	0.02	0.01
SD	0.20	2.68	2.85	0.10	0.47	0.45	0.05	0.07	0.08	0.04	0.06	0.06
Min.	0.12	-8.54	-8.43	-0.13	-0.21	-0.11	-0.19	-0.04	-0.13	-0.10	-0.07	-0.11
Max.	0.86	6.19	6.72	0.21	2.13	2.01	0.03	0.25	0.12	0.06	0.15	0.13
Range	0.75	14.73	15.15	0.34	2.35	2.12	0.21	0.29	0.25	0.15	0.22	0.24
Total net heave[b]			10.56			2.39			0.23			0.30
Total vertical strain (%)[c]			2.35			0.53			0.05			0.07

[a] Net heave = freezing period heave minus thawing period heave; determined where values of heave during both freezing period and thawing period of a freeze-thaw cycle are available.

[b] Overall change in elevation of top of unfrozen block measured during successive cycles of net heave. Note that heave was not measured during freezing period 1.

[c] Represents total vertical strain of block in unfrozen condition over the course of the experiment, except for freezing period 1 and thawing period 22, for which no data were recorded.

Table S2 Heave and settlement of blocks U1 to U6 during freezing periods ('Freeze') and thawing periods ('Thaw') of the unidirectional freezing experiment

	U1 Heave (mm)			U2 Heave (mm)			U3 Heave (mm)			U4 Heave (mm)			U5 Heave (mm)			U6 Heave (mm)		
Cycle	**Freeze**	**Thaw**	**Net** [a]	**Freeze**	**Thaw**	**Net**	**Freeze**	**Thaw**	**Net**	**Freeze**	**Thaw**	**Net**	**Freeze**	**Thaw**	**Net**	**Freeze**	**Thaw**	**Net**
1	1.59	-1.54	0.05	1.84	-1.84	0.00	-0.06	0.09	0.03	0.00	0.00	0.00	-0.17	0.14	-0.03	-0.09	0.00	-0.09
2	1.45	-1.53	-0.08	1.90	-1.95	-0.06	-0.42	0.23	-0.19	-0.14	-0.09	-0.23	-0.25	0.29	0.03	-0.10	-0.03	-0.14
3	1.25	-1.22	0.03	1.39	-1.45	-0.06	-0.15	0.23	0.08	0.04	0.10	0.14	-0.25	0.30	0.05	0.00	0.14	0.14
4	1.24	-1.33	-0.09	1.70	-1.72	-0.02	-0.17	0.12	-0.06	0.04	-0.12	-0.08	-0.25	0.15	-0.10	-0.16	0.06	-0.10
5	1.24	-1.37	-0.14	1.45	-1.59	-0.14	-0.17	0.09	-0.08	0.08	-0.16	-0.08	-0.15	0.15	0.00	-0.11	0.14	0.02
6	1.14	-1.16	-0.02	1.36	-1.55	-0.19	-0.09	0.12	0.02	0.26	-0.17	0.08	-0.12	0.17	0.06	-0.06	0.14	0.08
7	1.08	-1.17	-0.09	1.26	-1.23	0.02	-0.06	0.09	0.03	0.17	-0.20	-0.02	-0.25	0.20	-0.06	-0.22	0.22	0.00
8	0.83	-0.95	-0.11	1.14	-1.28	-0.14	-0.11	0.16	0.05	0.22	0.04	0.26	-0.12	0.20	0.08	-0.16	0.20	0.04
9	1.04	-0.98	0.06	1.31	-1.43	-0.11	-0.10	0.06	-0.05	-0.15	-0.02	-0.18	-0.25	0.28	0.02	-0.17	0.20	0.02
10	1.00	-1.06	-0.06	1.37	-1.23	0.14	-0.03	0.11	0.08	0.00	0.14	0.14	-0.22	0.31	0.09	-0.22	0.33	0.11
11	0.95	-1.03	-0.08	1.20	-1.28	-0.08	-0.11	0.00	-0.11	0.08	-0.08	0.00	-0.35	0.29	-0.06	-0.17	0.09	-0.08
12	1.08	-1.22	-0.14	1.53	-1.59	-0.06	0.00	0.00	0.00	0.06	0.00	0.06	-0.17	0.20	0.02	-0.03	0.11	0.08
13	0.78 [b]	-0.72	0.06	0.95 [b]	-1.00	-0.06	0.00 [b]	-0.02	-0.02	-0.02 [b]	-0.18	-0.20	-0.20 [b]	0.20	0.00	-0.08 [b]	0.02	-0.06
14	0.97	-0.97	0.00	1.20	-1.26	-0.06	-0.04	-0.08	-0.12	0.12	0.00	0.12	-0.16	0.14	-0.02	-0.08	0.14	0.06
15	0.83	-0.87	-0.03	1.18	-1.14	0.03	0.12	-0.04	0.08	0.02	0.04	0.06	-0.20	0.20	0.00	-0.11	0.11	0.00
16	0.92	-0.87	0.06	1.16	-1.20	-0.03	0.04	-0.04	0.00	0.08	-0.08	0.00	-0.14	0.20	0.06	-0.08	0.06	-0.02
17	0.81	-0.83	-0.02	1.35	-1.26	0.09	-0.08	0.14	0.06	0.05	-0.08	-0.04	-0.23	0.23	0.00	-0.03	0.06	0.02
18	0.91	-0.89	0.02	1.36	-1.39	-0.03	-0.12	0.09	-0.02	-0.02	0.08	0.06	-0.17	0.06	-0.12	-0.06	0.08	0.02
19	1.14	-1.03	0.11	1.64	-1.45	0.19	-0.09	0.09	0.00	0.02	-0.02	0.00	-0.12	0.14	0.02	-0.14	0.09	-0.05
20	-0.06 [b]	-0.06	-0.11	0.09 [b]	0.02	0.11	-0.12 [b]	0.17	0.06	-0.12 [b]	0.14	0.02	-0.02 [b]	0.02	0.00	0.02 [b]	0.12	0.14
21	1.33	-1.24	0.09	1.93	-1.79	0.14	-0.11	0.08	-0.03	-0.05	0.05	0.00	-0.16	0.16	0.00	-0.17	0.06	-0.12
22	1.22	-1.12	0.10	1.87	-1.72	0.15	-0.12	0.23	0.11	-0.02	0.08	0.06	-0.16	0.28	0.12	-0.11	0.17	0.06
23	1.48	-1.43	0.06	2.19	-2.03	0.16	-0.23	0.23	0.00	-0.06	-0.02	-0.08	-0.22	0.25	0.04	-0.17	0.14	-0.04
24	1.51	-1.33	0.17	2.65	-2.42	0.23	-0.11	0.08	-0.03	0.00	0.12	0.12	-0.35	0.35	0.00	-0.16	0.16	0.00
25	1.53	-1.47	0.06	2.56	-2.15	0.41	-0.14	0.17	0.03	-0.09	0.00	-0.09	-0.25	0.16	-0.09	-0.14	0.17	0.04
26	1.14	-1.06	0.08	1.90	-1.80	0.09	-0.17	0.12	-0.06	0.09	-0.09	0.00	-0.02	0.06	0.03	-0.25	0.28	0.02
27	2.18			2.53			-0.20			-0.11			-0.25			-0.25		
Mean	1.13	-1.09	0.00	1.56	-1.49	0.03	-0.11	0.10	-0.01	0.02	-0.02	0.00	-0.19	0.20	0.01	-0.12	0.12	0.01
SD	0.39	0.31	0.09	0.55	0.46	0.14	0.10	0.09	0.07	0.10	0.10	0.11	0.08	0.08	0.06	0.07	0.08	0.07
Min.	-0.06	-1.54	-0.14	0.09	-2.42	-0.19	-0.42	-0.08	-0.19	-0.15	-0.20	-0.23	-0.35	0.02	-0.12	-0.25	-0.03	-0.14
Max.	2.18	-0.06	0.17	2.65	0.02	0.41	0.12	0.23	0.11	0.26	0.14	0.26	-0.02	0.35	0.12	0.02	0.33	0.14
Range	2.23	1.48	0.31	2.56	2.44	0.61	0.54	0.31	0.31	0.41	0.34	0.49	0.32	0.32	0.23	0.28	0.37	0.28
Total net heave [c]			-0.03			0.73			-0.14			0.11			0.14			0.16
Total vertical strain (%) [d]			-0.01			0.16			-0.03			0.02			0.03			0.04

[a] Net heave = freezing period heave minus thawing period heave; determined where values of heave during both freezing period and thawing period of a freeze-thaw cycle are available.

[b] Approximate value because some data are missing.

[c] Overall change in elevation of top of unfrozen block measured during successive cycles of net heave.

[d] Represents total vertical strain of block in unfrozen condition over the course of the experiment, except for thawing period 27, for which n o data were recorded.